

Published in final edited form as:

Chem Res Toxicol. 2010 April 19; 23(4): 788–801. doi:10.1021/tx900436m.

A Comprehensive Approach to the Profiling of the Cooked Meat Carcinogens 2-Amino-3,8-dimethylimidazo[4,5-*f*]quinoxaline, 2-Amino-1-methyl-6-phenylimidazo[4,5-*b*]pyridine and their Metabolites in Human Urine

Dan Gu¹, Lynn McNaughton², David LeMaster², Brian G. Lake³, Nigel J. Gooderham⁴, Fred F. Kadlubar⁵, and Robert J. Turesky¹

¹Division of Environmental Health Sciences, New York State Department of Health, Albany, New York 12201

²Division of Translational Medicine, Wadsworth Center, New York State Department of Health, Albany, New York 12201

³ Centre for Toxicology, Health and Medical Sciences, University of Surrey, GU2 7XH, UK and LFR Molecular Sciences, Randalls Road, Leatherhead, Surrey, KT22 7RY, UK

⁴Biomolecular Medicine, Faculty of Medicine, Imperial College London, Sir Alexander Fleming Building, London SW7 2AZ, United Kingdom.

⁵ Winthrop P. Rockefeller Cancer Institute, University of Arkansas for Medical Sciences, Little Rock, AR 72205

Abstract

A targeted liquid chromatography/tandem mass spectrometry-based metabolomics-type approach, employing a triple stage quadrupole mass spectrometer in the product ion scan and selected reaction monitoring modes, was established to profile 2-amino-3,8-dimethylimidazo[4,5-*f*]quinoxaline (MeIQx), 2-amino-1-methyl-6-phenylimidazo[4,5-*b*]pyridine (PhIP), and their principal metabolites in urine of omnivores. A mixed-mode reverse phase cation exchange resin enrichment procedure was employed to isolate MeIQx, and its oxidized metabolites, 2-amino-8-(hydroxymethyl)-3-methylimidazo[4,5-*f*]quinoxaline (8-CH₂OH-IQx) and 2-amino-3-methylimidazo[4,5-*f*]quinoxaline-8-carboxylic acid (IQx-8-COOH), which are produced by cytochrome P450 1A2 (P450 1A2). The phase II conjugates *N*²-(β-1-glucosiduronyl)-2-amino-3,8-dimethylimidazo[4,5-*f*]quinoxaline and *N*²-(3,8-dimethylimidazo[4,5-*f*]quinoxalin-2-yl)-sulfamic acid were measured indirectly, following acid hydrolysis to form MeIQx. The enrichment procedure permitted the simultaneous analysis of PhIP; *N*²-(β-1-glucosiduronyl)-2-amino-1-methyl-6-phenylimidazo[4,5-*b*]pyridine; *N*³-(β-1-glucosiduronyl)-2-amino-1-methyl-6-phenylimidazo[4,5-*b*]pyridine; 2-amino-1-methyl-6-(4'-hydroxy)-phenylimidazo[4,5-*b*]pyridine (4'-HOPhIP); and the isomeric *N*²- and *N*³-glucuronide conjugates of the carcinogenic metabolite,

Correspondence to: Robert J. Turesky.

CORRESPONDING AUTHOR FOOTNOTE: To whom correspondence should be addressed: Tel 518-474-4151. Fax 518-473-2095. Rturesky@wadsworth.org.

SUPPORTING INFORMATION PARAGRAPH

¹H NMR chemical shift data (ppm) for PhIP-*N*-glucuronides (Table S-1); Performance of the analytical method for PhIP and its metabolites (Table S-2); 2D-¹H-¹H COSY NMR spectra of PhIP-*N*²-Gl (Figure S-1A) and PhIP-*N*³-Gl (Figure S-1B and S-1C); Calibration curves of MeIQx and its metabolites (Figure S-2A – S-2C); PhIP and its metabolites (Figure S-3A – S-3D); and LC-ESI/MS/MS traces of MeIQx, PhIP, and 4'-HO-PhIP in urine of an omnivore, before and after acid hydrolysis of urine (Figure S-4), are shown in Supporting Information. This material is available free of charge via the Internet at <http://pubs.acs.org>.

2-hydroxyamino-1-methyl-6-phenylimidazo[4,5-*b*]pyridine (HONH-PhIP), which is formed by P450 1A2. The limit of quantification (LOQ) for MeIQx, PhIP, and 4'-HO-PhIP was ~5 pg/mL; the LOQ values for 8-CH₂OH-IQx and IQx-8-COOH were, respectively, <15 pg/mL and <25 pg/mL; and the LOQ values for the glucuronide conjugates of PhIP and HONH-PhIP were 50 pg/mL. The metabolism was extensive: Less than 9% of the dose was eliminated in urine as unaltered MeIQx and <1% was eliminated as unaltered PhIP. Phase II conjugates of the parent amines accounted for up to 12% of the dose of MeIQx, and up to 2% of the dose of PhIP. 8-CH₂OH-IQx and IQx-8-COOH accounted for up to 76% of the dose of MeIQx, and the isomeric glucuronide conjugates of HONH-PhIP accounted for up to 33% of the dose of PhIP that were eliminated in urine within 10 hours of meat consumption. P450 1A2 significantly contributes to the metabolism of both HAAs, but with marked differences in substrate specificity. P450 1A2 primarily catalyzes the detoxification of MeIQx by oxidation of the 8-methyl group, whereas it catalyzes the bioactivation of PhIP by oxidation of the exocyclic amine group.

INTRODUCTION

Urine is a useful biological matrix for the assessment of recent exposures to carcinogens, since large quantities can be obtained noninvasively. Moreover, the characterization of the urinary metabolic profiles of the genotoxicants can provide an estimate of the relative extent of bioactivation, as opposed to detoxification, undergone by the chemicals *in vivo* (1). These measurements can also reveal inter-individual differences in metabolism due to genetic polymorphisms that code for enzymes involved xenobiotic metabolism; such differences can affect the genotoxic potency of many procarcinogens. A number of biomarkers of carcinogens present in tobacco smoke (1), as well as biomarkers of the hepatocarcinogen aflatoxin B₁ (2,3), have been measured in human urine.

The measurement of urinary biomarkers of carcinogens can also be used to assess the efficacy of chemoprotective agents in modulating the activities of phase I and II enzymes involved in carcinogen metabolism (4,5). This is an area of research that we are currently investigating and involves heterocyclic aromatic amines (HAAs), a class of carcinogens formed in high-temperature-cooked meats (6).

2-Amino-3,8-dimethylimidazo[4,5-*f*] quinoxaline (MeIQx) and 2-amino-1-methyl-6-phenylimidazo[4,5-*b*]pyridine (PhIP) are two of the most mass-abundant carcinogenic heterocyclic aromatic amines (HAAs) formed in cooked meats: Concentrations can range from less than 1 part per billion (ppb) to greater than 15 ppb in meats prepared under common household cooking conditions (7). Both compounds induce tumors in multiple organs of rodents during long-term feeding studies (6). Putative DNA adducts of MeIQx (8) and PhIP (9-12) have been detected in human tissues. Thus, the chronic consumption of foods containing these HAAs constitutes a potential human health hazard: the Report on Carcinogens, Eleventh Edition, of the National Toxicology Program, concluded that several prevalent HAAs, including MeIQx and PhIP, are "reasonably anticipated" to be human carcinogens (13).

The metabolism of MeIQx and PhIP has been extensively studied *in vitro* with tissue fractions, purified and recombinant enzymes (14-17), and hepatocytes (18,19), as well as *in vivo* in experimental laboratory animals (18,20-22), and in humans (5,23-28). The major pathways of metabolism of MeIQx and PhIP are depicted in Schemes 1 and 2. Metabolic activation occurs by cytochrome P450 mediated N-oxidation of the exocyclic amine group, to produce 2-hydroxyamino-3,8-dimethylimidazo[4,5-*f*]quinoxaline (HONH-MeIQx) and 2-hydroxyamino-1-methyl-6-phenylimidazo[4,5-*b*]pyridine (HONHPhIP). This oxidation step is catalyzed primarily by P450 1A2 in liver and by P450s 1A1 and 1B1 in extrahepatic

tissues (16,17). The HONH-HAAs undergo further metabolism by *N*-acetyltransferases (NATs) or by sulfotransferases (SULTs), to produce highly reactive esters that bind to DNA (29).

Competing pathways of metabolism serve as mechanisms of detoxification for both HAAs. In the case of MeIQx, P450 1A2 also catalyzes oxidation of the 8-CH₃ group to form 2-amino-8-(hydroxymethyl)-3-methylimidazo[4,5-*f*]quinoxaline (8-CH₂OH-IQx), which undergoes further oxidation by P450 1A2, to form 2-amino-3-methylimidazo[4,5-*f*]quinoxaline-8-carboxylic acid (IQx-8-COOH) (30). This latter metabolite is the major detoxification product of MeIQx in human hepatocytes (31), and in humans (23). It is noteworthy that IQx-8-COOH is not formed in rodents or nonhuman primates (21,31). Human P450s catalyze oxidation at the 4' position of the phenyl ring of PhIP, to form 2-amino-1-methyl-6-(4'-hydroxy)-phenylimidazo[4,5-*b*]pyridine (4'-HO-PhIP); however, the rates of formation of 4'-HO-PhIP are significantly lower than the rates of HONH-PhIP formation (16,22,32). Although 4'-HO-PhIP is a minor metabolic product of human P450 1A2, it is a principal detoxification product of PhIP in rodents and non-human primates (18,21).

MeIQx and PhIP also undergo detoxification by phase II conjugation reactions. MeIQx undergoes sulfamation, to form *N*²-(3,8-dimethylimidazo[4,5-*f*]quinoxalin-2-yl)-sulfamic acid (MeIQx-*N*²-SO₃H), the process is catalyzed by sulfotransferase 1A1 (SULT1A1) (33). A second phase II metabolite of MeIQx is the glucuronide conjugate, *N*²-(β-1-glucosiduronyl)-2-amino-3,8-dimethylimidazo[4,5-*f*]quinoxaline (MeIQx-*N*²-G1), which is formed by uridine diphosphate glucuronosyltransferases (UGTs), apparently UGT1A isoforms (34-36). An *N*²-glucuronide conjugate of HONH-MeIQx has been characterized as *N*²-(β-1-glucosiduronyl)-2-hydroxyamino-3,8-dimethylimidazo[4,5-*f*]quinoxaline (HON-MeIQx-*N*²-G1) (37). Both PhIP and HNOH-PhIP undergo conjugation by UGT1A isoforms to produce *N*²- and *N*³-glucuronide conjugates (34-36). The glucuronide conjugates of HNOH-MeIQx and HONH-PhIP are viewed as detoxification products (27).

The analysis of unaltered MeIQx and PhIP, and their metabolites, in human urine is an analytical challenge, because usually only ~1 to several μg of each compound is ingested per day, in individuals eating well-done meat (38). Thus, the concentrations of these HAAs and their metabolites are often well below the ppb level in urine. The polar and ionic nature of the metabolites also presents difficulties for their isolation along with their parent HAAs, from thousands of other components in the urine matrix. Various analytical approaches have been devised to isolate MeIQx or PhIP from human urine: such techniques have included solvent extraction (39,40), solid-phase extraction (SPE) (41), use of molecularly imprinted polymers (28), and immunoaffinity methods (24), followed by quantification by gas chromatography and negative ion chemical ionization mass spectrometry (GC-NICI-MS) (39,40,42), or LC-ESI/MS/MS (28,41), or alternatively followed by fluorescence detection (25). [¹⁴C]-MeIQx, [¹⁴C]-PhIP, and [¹⁴C]-radiolabeled metabolites have been identified in human urine by accelerator mass spectrometry (AMS) (23,27,43). Urinary metabolites have also been detected by liquid chromatography-electrospray ionization/mass spectrometry/tandem mass spectrometry (LCESI/MS/MS) (5,26), or indirectly, after chemical reduction or acid hydrolysis of HONH-PhIP conjugates, with detection LC-ESI/MS/MS or GC-NICI-MS (44,45).

To our knowledge, no report in the literature has described the simultaneous analysis of MeIQx and PhIP, and their principal metabolites, in human urine. The concurrent analysis of these biomarkers is important since the urinary excretion levels of either MeIQx or PhIP can only serve as an approximate measure for one another, in assessment of exposures in humans consuming unrestricted diets (46). Moreover, assessment of the efficacies of

chemoprotective agents requires a multipurpose analytical method that can be employed to quantitate both HAAs and their metabolites in urine. We recently reported a facile solid phase extraction (SPE) method to isolate PhIP and several of its major metabolites in human urine; its use is followed by quantitative measurements by LC/MS (47). In this article, we describe a refinement of the SPE procedure to create a rapid, one-step method to isolate MeIQx and PhIP, and several of their P450 1A2-derived metabolites in urine, followed by quantitative LC-ESI/MS/MS analysis. With this validated method, we have examined the interrelationship between the oxidative metabolism of MeIQx and that of PhIP, in urine samples from 10 volunteers.

EXPERIMENTAL PROCEDURES

Caution: MeIQx, PhIP, and several of their derivatives are potential human carcinogens and should be handled with caution in a well-ventilated fume hood with the appropriate protective clothing.

Materials and Methods

MeIQx, PhIP, and 2-amino-3-trideutromethyl-8-methylimidazo[4,5-*f*]quinoxaline ($[^2\text{H}_3\text{C}]$ -MeIQx) and 2-amino-1-trideutromethyl-6-phenylimidazo[4,5-*b*]pyridine ($[^2\text{H}_3\text{C}]$ -PhIP) (both at 99% isotopic purity) were purchased from Toronto Research Chemicals (Toronto, ON, Canada). NADPH, NADH, glucose-6-phosphate, uridine-5'-diphosphoglucuronic acid (UDPGA), glucose-6-phosphate dehydrogenase, alamethicin, β -glucuronidase Type IX-A from *E. coli*, and sulfatase from abalone entrails Type VIII, were all purchased from Sigma (St. Louis, MO). Pooled male rabbit liver microsomes (New Zealand White) were purchased from BD Biosciences (Woburn, MA). Male SD rat liver microsomes of animals pretreated with polychlorinated biphenyls (PCBs, Aroclor-1254) were obtained from Moltox (Boone, NC). Human liver microsomal samples were from Tennessee Donor Services, Nashville, TN, and were a gift kindly provided by Dr. F. P. Guengerich, Vanderbilt University. The P450 1A2 protein expression and metabolic activity were previously characterized (16). All solvents used were high-purity B & J Brand® from Honeywell Burdick and Jackson (Muskegon, MI). ACS reagent grade HCO_2H (88%) was purchased from J.T. Baker (Phillipsburg, NJ), Retain CX resins (30 mg) were purchased from ThermoFisher Scientific (Palm Beach, FL), and Baker C18 solid-phase extraction (SPE) resins (500 mg) were purchased through Krackeler Scientific Inc. (Albany, NY). All other chemical reagents were ACS grade, and purchased from Sigma Aldrich.

General Methods

Mass spectra of synthetic and biosynthetic derivatives were obtained on a Finnigan Quantum Ultra triple stage quadrupole mass spectrometer (Thermo Electron, San Jose, CA). Typical instrument tuning parameters were: capillary temperature 275 °C, source spray voltage 3.5 kV, sheath gas setting 35, tube lens offset 95, capillary offset 35, and source fragmentation 15 V. Argon, set at 1.5 mTorr, was used as the collision gas. Analyses were conducted in positive ionization mode. NMR-resonance experiments assignment experiments were carried out at 25°C and 45°C for the rabbit and human liver PhIP-*N*-glucuronides, respectively, on a Bruker Avance DRX 600 MHz spectrometer equipped with a triple resonance cryoprobe (Bruker BioSpin Corporation, Billerica, MA). The ^1H chemical shifts were referenced directly from the DMSO-*d*₆ multiplet at 2.50 ppm. A standard DQF-COSY experiment was employed to collect 1024 t_1 increments over a 7507 Hz spectral window. Selected NMR spectra are provided in the Supporting Information. HPLC separations of biomarkers were done with an Agilent (Palo Alto, CA) Model 1100 HPLC system equipped with a photodiode array detector, equipped with a Rheodyne 7725i (Rhonert Park, CA) manual injector.

Syntheses

2-Amino-3-methylimidazo[4,5-f]quinoxaline-8-carbaldehyde, 8-CH₂OH-IQ_x, IQ_x-8-COOH, and MeIQ_x-N²-SO₃H

MeIQ_x (5 mg, 2.3 μmol) in dioxane (20 mL), was oxidized with selenium dioxide (5 mg, 45 μmol), by heating the solution at reflux for 5 h, as previously described (31). The two major products, the 8-carbaldehyde derivative of MeIQ_x and IQ_x-8-COOH, were formed in approximately 30 and 60% yields, respectively. Treatment of the reaction mixture with NaCNBH₃ (5 mg, 78 μmol, 1 h at 37 °C) resulted in complete reduction of the aldehyde to 8-CH₂OH-IQ_x (31). MeIQ_x-N²-SO₃H was prepared by treatment of MeIQ_x with a 1.2 mol excess of chlorosulfonic acid in anhydrous pyridine, as previously described (48).

Biosynthesis of NOH-MeIQ_x-N²-GI and MeIQ_x-N²-GI

These metabolites were prepared by incubating MeIQ_x or HONH-MeIQ_x (0.5 mM) (or [²H₃C]-MeIQ_x, [²H₃C]-HONH-MeIQ_x) with 20 mg of liver microsomal protein from rats pretreated with PCBs in 10 mL of 100 mM Tris-HCl buffer (pH 7.5), containing 10 mM MgCl₂, and UDPGA (5 mM) for 6 h at 37 °C (49). The microsomal mixture was preincubated with alamethicin (50 μg/mg protein) on ice for 15 min, prior to addition of the MeIQ_x compounds. The glucuronide metabolites were isolated as previously described (47). HONH-MeIQ_x was synthesized as previously described (50).

Biosynthesis of 4'-HO-PhIP, N²-(β-1-glucosiduronyl)-2-amino-1-methyl-6-phenylimidazo[4,5-b]pyridine (PhIP-N²-GI), N³-(β-1-glucosiduronyl)-2-amino-1-methyl-6-phenylimidazo[4,5-b]pyridine (PhIP-N³-GI), N²-(β-1-glucosiduronyl)-N-hydroxy-2-amino-1-methyl-6-phenylimidazo[4,5-b]pyridine (HON-PhIP-N²-GI) and N³-(β-1-glucosiduronyl)-N-hydroxy-2-amino-1-methyl-6-phenylimidazo[4,5-b]pyridine (HON-PhIP-N³-GI) Conjugates

The biosynthesis of PhIP-N²-GI was carried out with rabbit liver microsomal protein (1 mg/mL), and the biosynthesis of PhIP-N³-GI was done with human liver microsomal protein (2 mg/mL) in 100 mM Tris-HCl buffer (pH 7.5), containing 10 mM MgCl₂, PhIP (0.5 mM), and UDPGA (5 mM). The mixture was preincubated with alamethicin (50 μg/mg protein) on ice for 15 min, followed by incubation at 37 °C for 6 h. The products were isolated as previously described (47). The isomeric HON-PhIP-N²-GI and HON-PhIP-N³-GI metabolites were prepared from human or rat liver microsomes as previously described (47). 4'-HOPhIP was produced from the oxidation of PhIP with rat liver microsomes pretreated with PCBs (47).

Human Subjects and Meat Consumption

The analyses of MeIQ_x and PhIP metabolites were conducted on urine samples from male volunteers who participated in a previous investigation; and full details were reported previously (5,51). In brief, each subject consumed 275 g of cooked minced beef patties that had been fried without added oil or fat for 6 min on each side, using a hot metal griddle at 300 °C, until the meat was well-browned. The average amount of MeIQ_x ingested was 920 ng, and the average amount of PhIP ingested was 4,950 ng (51). A urine collection was then commenced over 10 h, and urine samples were stored at -80 °C. A subset of samples were sent blind coded on dry ice to the Wadsworth Center for further analyses. This study was approved by the Institutional Review Board at the Wadsworth Center.

Solid-phase Extraction (SPE) of MeIQ_x and PhIP and their Metabolites from Urine

The enrichment procedure was previously reported (47). In this present work-up, the organic precipitation and vacuum concentration steps were omitted prior to SPE. The urine samples (1.0 mL) were acidified with HCO₂H (88% v/v, 20 μL) and centrifuged at 15,000 g for 2

min, to remove particulates. The supernatants were applied to ThermoFisher HyperSep Retain CX (30 mg resin) cartridges that had been prewashed with CH₃OH containing 5% NH₄OH (1 mL), followed by 2% HCO₂H in H₂O (1 mL). The resins were attached to a vacuum manifold, under slight positive pressure (~5 inches of Hg), to achieve a flow rate of the eluent of approximately 1 mL/min. After application of the samples, the cartridges were washed with 2% HCO₂H in H₂O (1 mL), followed by 2% HCO₂H in CH₃OH (1 mL), H₂O (1 mL) and 5% NH₄OH (1 mL). The resin was allowed to run to dryness. Next, the biomarkers were eluted from the resin with CH₃OH containing 1% NH₄OH (1.5 mL). This solvent was allowed to absorb into the resin for 3 min, prior to gentle manual elution of the solvent with a disposable 1 mL syringe. The extract was collected into Eppendorf tubes (2.0 mL), and placed in a ventilated hood for 15 min to allow the NH₃ to evaporate. The extracts were concentrated to approximately 0.1 mL, by vacuum centrifugation. Then, the samples were transferred into silylated glass conical vials (0.35 mL volume) from MicroLiter Analytical Supplies, Inc. (Suwanee, GA) and evaporated to dryness by vacuum centrifugation. The samples were resuspended in 1:1 H₂O:DMSO (20 μ L).

LC-ESI/MS/MS Analyses

Chromatography was performed with an Agilent 1100 series capillary LC system (Agilent Technologies, Palo Alto, CA) equipped with an Agilent Zorbax-SB-C18 column (0.3 \times 250 mm; 5 μ m particle size). Analytes were separated by a gradient. The A solvent contained 0.01% HCO₂H in H₂O, and the B solvent contained 0.01% HCO₂H and 5% H₂O in CH₃CN. The flow rate was set at 6 μ L/min, starting at 100% A and holding for 1 min, followed by a linear gradient to 60% B at 35 min, and then to 100% B at 36 min, and holding for 4 min. The gradient was reversed to the starting conditions over 1 min, and a post-run time of 14 min was required for re-equilibration. The mass-spectral data were acquired on a FinniganTM Quantum Ultra Triple Stage Quadrupole MS; data manipulations were carried out with Xcalibur version 2.07 software. Analyses were conducted in the positive ionization mode and employed an Advance nanospray source from Michrom Bioresources Inc. (Auburn, CA). The spray voltage was set at 2100 V; the in-source fragmentation was -10 V; and the capillary temperature was 220 $^{\circ}$ C. No sheath or auxiliary gas was used. The peak widths (in Q1 and Q3) were set at 0.7 Da, and the scan width was 0.002 Da.

The following transitions and collision energies were used for the quantification of MeIQx, PhIP, and their metabolites: MeIQx and [²H₃C]-MeIQx: 214.1 \rightarrow 199.1 and 217.1 \rightarrow 199.1, at 30 eV; 8-CH₂OH-IQx and [²H₃C]-8-CH₂OH-IQx: 230.1 \rightarrow 212.1, 197.1 and 233.1 \rightarrow 215.1, 197.1, at 20 or 30 eV; 8-COOH-IQx and [²H₃C]-8-COOH-IQx: 244.1 \rightarrow 198.1, 183.1 and 247.1 \rightarrow 201.1, 183.1, at 20 or 30 eV; PhIP and [²H₃C]-PhIP: 225.1 \rightarrow 210.1 and 228.1 \rightarrow 210.1 at 33 eV; 4'-HO-PhIP: 241.1 \rightarrow 226.1 at 35 eV; isomeric PhIP-*N*-Gl and [²H₃C]-PhIP-*N*-Gl: 401.1 \rightarrow 210.1 and 404.1 \rightarrow 210.1 at 55 eV; isomeric HON-PhIP-*N*-Gl and [²H₃C]-HON-PhIP-*N*-Gl: 417.1 \rightarrow 225.1 and 223.1 and 420.1 \rightarrow 228.1 and 225.1 @ 34 eV. The dwell time for each transition was 10 ms. Argon was used as the collision gas and was set at 1.5 mTorr. Product ion spectra were acquired on the protonated molecules [M + H]⁺, scanning from *m/z* 50 to 500 at a scan speed of 250 amu/s using the same acquisition parameters as above.

Calibration Curves

Calibration curves were generated in triplicate by the addition of a fixed amount of [²H₃C]-PhIP and [²H₃C]-MeIQx (100 pg), and [²H₃C]-8-CH₂OH-IQx (300 pg) and 0, 6, 12, 16, 20, 40, 60 or 100 pg of the unlabeled standards per 1.0 mL urine from a volunteer who had not consumed cooked meat for at least 48 h. [²H₃C]-IQx-8-COOH was added at a level of 300 pg/mL of urine, and the unlabeled standard was added at 0, 30, 60, 80, 100, 200, 300 or 500 pg per mL of urine. The calibration curves of PhIP metabolites were also constructed in

triplicate with [$^2\text{H}_3\text{C}$]-PhIP-*N*3-GI, [$^2\text{H}_3\text{C}$]-HON-PhIP-*N*²-GI, and [$^2\text{H}_3\text{C}$]-HON-PhIP-*N*3-GI added at a fixed concentration of 1000 pg per mL of urine, and the unlabeled analytes were each added at concentrations of 0, 60, 120, 160, 200, 400, 600, or 1000 pg/mL of urine. The calibration data were fitted to a straight line using the ordinary least-squares method with equal weightings. Each urine sample was subjected to the SPE processing conditions described above. The within-day and between-day precisions for MeIQx and PhIP and their metabolites were calculated in triplicate or quadruplicate as described (52), with use of urine samples from three different subjects collected during 10 hr, after consumption of cooked meat (5). The measurements were done on three different days over a time period of 1 month. The response of the signal of 4'-HO-PhIP was assumed to be comparable to PhIP and [$^2\text{H}_3\text{C}$]-PhIP was employed as an internal standard to estimate the levels of 4'-HO-PhIP.

Enzyme and Acid Hydrolysis Assays

Urine samples from meat-eaters (0.5 mL) were spiked with the isotopically labeled internal standards of MeIQx and PhIP, or their metabolites, and then diluted with 0.5 mL of 100 mM sodium acetate buffer (pH 5.5) or 0.5 mL of 100 mM sodium phosphate buffer (pH 6.5). Enzyme hydrolysis was conducted with β -glucuronidase (14 U/mL) and sulfatase (2 U/mL) at 37 °C for 4 h. The samples were then diluted with glacial acetic acid (1 mL) and processed by SPE. Urine samples (0.5 mL) were also subjected to acid hydrolysis in 50% (v/v) glacial acetic acid or in 1 N HCl, by heating at 80 °C for 8 h. Upon cooling, the samples were processed by SPE. Under these acid hydrolysis conditions, MeIQx-*N*²-SO₃H, MeIQx-*N*²-GI, and PhIP-*N*²-GI were quantitatively hydrolyzed to the parent amines, whereas the PhIP-*N*3-GI was stable and <5% of the conjugate underwent hydrolysis.

Statistical Analysis

Spearman's rank correlation coefficient (r_s) determinations for the urinary metabolites and unmetabolized HAAs were done with GraphPad Prism[®] Version 4 software (San Diego, CA).

Results

Rapid SPE and LC-ESI/MS/MS Analysis of MeIQx, 8-CH₂OH-MeIQx, IQx-8-COOH, PhIP, PhIP-*N*²-GI, 4'-HO-PhIP, HON-PhIP-*N*²-GI, and HON-PhIP-*N*3-GI in Urine of Omnivores

A facile SPE procedure previously developed to purify PhIP and its metabolites from urine (47) was employed for the concurrent isolation of MeIQx, 8-CH₂OH-MeIQx and IQx-8-COOH. We determined that the treatment of urine with an organic solvent, to precipitate salt and protein, and the ensuing vacuum concentration step, to remove the organic solvent, are not required prior to SPE. The recovery of the analytes, the purity of the extracts, and the limit of quantification (LOQ) of MeIQx, PhIP, and their metabolites were not affected by the omission of these pre-SPE processing steps. The exclusion of these procedures has resulted in a rapid, one-step, high-throughput method for isolation of these HAA urinary biomarkers.

The analyses of MeIQx, 8-CH₂OH-MeIQx, and IQx-8-COOH in urine from an omnivore who had refrained from eating cooked meat for 48 h (pre-exposure) and in urine collected over a 10 h time point, after consumption of grilled meat (post-exposure), is shown in Figure 1. The compounds were monitored by LC-ESI/MS/MS. The transition employed to monitor MeIQx ($[\text{M}+\text{H}]^+ \rightarrow [\text{M}+\text{H}-15]^{+\bullet}$ at 34 eV) produces a radical cation. The product ion arises by homolytic cleavage of the 3-*N*-CH₃ bond (53). The transition used to monitor 8-CH₂OH-IQx ($[\text{M}+\text{H}]^+ \rightarrow [\text{M}+\text{H}-18]^+$ at 20 eV) is due to the loss of H₂O from the alcohol group (30). The transition employed to monitor IQx-8-COOH ($[\text{M}+\text{H}]^+ \rightarrow [\text{M}+\text{H}-46]^+$ at 20 eV) is attributed to loss of H₂O and CO (30). These collision energy values provided the maximum

sensitivity in the selective reaction monitoring (SRM) mode. MeIQx was not detected in the pre-exposure urine sample, but it and its linear, tricyclic ring isomer, 2-amino-1,7-dimethylimidazo[4,5-g]quinoxaline (MeIQx) (54) were observed in urine collected after meat consumption by the subject (Figure 1). The internal standard [²H₃C]-8-CH₂OH-IQx was discerned in both pre- and post-exposure urine extracts; however, the background signal of the transition employed to monitor 8-CH₂OH-IQx was elevated in the pre-exposure urine, and numerous isobaric interfering peaks were observed in the urine extract after meat consumption. The transitions employed to measure IQx-8-COOH and [²H₃C]-IQx-8-COOH were even less selective. The internal standard was barely resolved from interfering peaks in the urine extract analyzed after meat consumption.

The Finnigan™ Quantum Ultra triple stage quadrupole MS has the capability of scanning at enhanced resolution, thereby increasing the mass resolving power from ~500 (m/Δm at full width at half maximum (FWHM) peak height), when it is scanning at 0.7 Da in either Q1 or Q3 (55), to a resolution of ~2000 for MeIQx and its oxidized metabolites, when the scan width is set at 0.1 Da at FWHM resolution. However, the use of the enhanced resolution scan mode did not significantly improve the signal to noise for the transitions of 8-CH₂OH-IQx, 8-IQx-8-COOH or their internal standards (data not shown).

The collision energy used to fragment these oxidized metabolites of MeIQx was then increased from 20 to 30 eV. Under the higher collision energy conditions, both metabolites undergo a second fragmentation at the 3-N-CH₃ bond and lose a CH₃ radical (30). Although the response of the signals was decreased at 30 eV, there was a dramatic diminution in the background signals at all transitions ([M+H]⁺ → ([M+H-33]⁺ and [M+H]⁺ → ([M+H-36]⁺ for 8-CH₂OH-IQx and [²H₃C]-8-CH₂OH-IQx, respectively; and [M+H]⁺ → ([M+H-61]⁺ and [M+H]⁺ → ([M+H-64]⁺ for IQx-8-COOH and [²H₃C]-IQx-8-COOH, respectively): at 30 eV, the target compounds and internal standards of both metabolites appear as distinct peaks (Figure 2). 8-CH₂OH-IQx or 8-IQx-8-COOH were not detected in the pre-dose urine extract, but both metabolites were readily discernible in the urine sample after meat consumption. Remarkably, the high sensitivity provided by the Quantum Ultra triple quadrupole MS with the Michrome Advance nanospray source has enabled us to acquire good-quality product ion spectra of the urinary 8-CH₂OH-IQx and IQx-8-COOH metabolites. The spectra are in good agreement with the spectra of the reference compounds (Figure 3) (30). The product ion spectra of MeIQx and MeIQx were also successfully acquired on urine samples that underwent acid-hydrolysis, resulting in an increase in the concentrations of these HAAs by up to 5-fold (*vide infra*) (Figure 4).

The analyses of PhIP, 4'-HO-PhIP, PhIP-N²-G1, PhIP-N³-G1, HON-PhIP-N²-G1, and HON-PhIP-N³-G1 in urine of the subject, pre- and post-meat consumption, are shown in Figure 5. None of these biomarkers were present in urine at detectable levels, when the subject had refrained from eating meat. However, PhIP and all of its metabolites, except for PhIP-N³-G1, were detected in the urine of the subject after consumption of meat. The product ion spectra of HON-PhIP-N²-G1 and HON-PhIP-N³-G1 are in excellent agreement to the spectra of the reference compounds previously published (data not shown) (47). Product ion spectra of PhIP and 4'-HO-PhIP were successfully acquired on urine samples that underwent acid hydrolysis: acid treatment increased the concentrations of these compounds by up to several-fold (*vide infra*) (Figure 6).

The relative amounts of isomeric glucuronide conjugates of PhIP formed by human liver microsomes *in vitro*, and their formation *in vivo*, based on urinary elimination, appear at variance. Human liver microsomes fortified with UDPGA produced 10-fold greater amounts of PhIP-N³-G1 than PhIP-N²-G1 (47,56), yet PhIP-N²-G1 is the main isomer known to be present in urine of meat eaters (Figure 5, t_R 27.1 min) (27,43). To confirm the sites of

conjugation and structural assignments of these isomeric glucuronide conjugates, we re-examined, by ^1H NMR spectroscopy, the human and rabbit liver microsomal PhIP-*N*-G1 metabolites: the glucuronide conjugate formed by rabbit liver was previously characterized as PhIP-*N*²-G1, whereas the conjugate produced by human liver was assigned as the PhIP-*N*³-G1 (56). Our ^1H NMR spectral data (Supporting Information, Figures S-1A – S-1C, and Table S-1), are consistent with the structures previously assigned: PhIP-*N*³-G1 is the major human liver microsomal metabolite, and PhIP-*N*²-G1 is the principal glucuronide conjugate produced by rabbit liver microsomes. Despite the strong preference, by human liver UGTs, to glucuronidate PhIP at the *N*³ imidazole atom, only the PhIP-*N*²-G1 isomer is eliminated in urine at levels above the limit of detection. However, the amounts of PhIP-*N*²-G1 eliminated in urine are low, and the direct glucuronidation of PhIP appears to be a minor route of detoxication of PhIP in these 10 subjects of our pilot study.

Performance of the Analytical Method

The recoveries of each internal standard [$^2\text{H}_3\text{C}$]-MeIQx and [$^2\text{H}_3\text{C}$]-PhIP (100 pg/mL); [$^2\text{H}_3\text{C}$]-8-CH₂OH-IQx and [$^2\text{H}_3\text{C}$]-IQx-8-COOH (each at 300 pg/mL); PhIP-*N*²-G1, HON-PhIP-*N*²-G1 and HON-PhIP-*N*³-G1 (each at 1000 pg/mL), added to urine prior to sample processing, were consistently between 40 and 80%, based on the response of the signals to those of pure standards measured by LCESI/MS/MS. The response of the signals of the processed internal standards is a function of the recoveries of the compounds and the potential ion suppression effects of the urine matrix (41). The calibration curves for MeIQx, 8-CH₂OH-IQx and IQx-8-COOH (generated from three independent replicates per calibrant level), constructed from urine samples from a subject who had refrained from eating cooked meat for 48 h, displayed good linearity ($R^2 > 0.997$) Supporting Information (Figure S-2). The calibration curves for PhIP, PhIP-*N*³-G1, HON-PhIP-*N*²-G1, and HON-PhIP-*N*³-G1 have previously been reported (47): the new sets of calibration curves of these biomarkers obtained in the current study are presented in the Supporting Information (Figure S-3). The LOQ values were derived based on a threshold of 10σ SD units above the background signal levels (57) in the urine samples from three volunteers, during the pre-exposure phase of the study. The LOQ values were ~5 pg/mL for MeIQx, PhIP, and 4'-HO-PhIP, whereas the LOQ for 8-CH₂OH-IQx was 10 pg/mL, and the LOQ for IQx-8-COOH was 35 pg/mL. The LOQ values for the glucuronide conjugates of PhIP and HONH-PhIP were estimated at 50 pg/mL.

The precision CV (%) of the estimates in the calibration curve at the lowest calibrant levels of MeIQx and 8-CH₂OH-IQx (6 pg/mL) was $\leq 11\%$, and the CV (%) for IQx-8-COOH at the lowest calibrant levels (30 pg/mL) was $\leq 10\%$; the precision values improved at the higher calibrant levels. The performance of the method was assessed by the within-day and between-day estimates and precision of measurements of MeIQx, 8-CH₂OH-IQx, IQx-8-COOH, PhIP-*N*²-G1, HON-PhIP-*N*²-G1, and HON-PhIP-*N*³-G1, in urine samples from three randomly selected volunteers determined over 3 separate days ($n = 3$ or 4 independent measurements per day), within a time period of 1 month. The results are summarized in Table 1. The within-day and between-day CV (%) in estimates of MeIQx, 8-CH₂OH-IQx, and IQx-8-COOH were well below 10.0%. The performance of the method was previously reported for PhIP and its *N*²- and *N*³-glucuronides of HONH-PhIP (47); a similar degree of precision is observed in these newly assayed urine samples (Table 1), and in the within-day and between-day CV (%) values, which are also below 10%, Supporting Information (Table S-2). Thus, the analytical method is precise, and intra-day and inter-day estimates for the quantification of MeIQx and PhIP, and their metabolites, are highly reproducible.

Estimation of MeIQx and PhIP Urinary Metabolites, and Correlations Among Urinary Metabolic Ratios (MRs)

The estimates of MeIQx and PhIP, and their metabolites in urine samples from 10 subjects are summarized in Table 2. Both HAAs underwent extensive metabolism: the proportion of unaltered MeIQx ranged from 2.2 to 8.7% of the ingested dose, whereas the proportion of unmetabolized PhIP ranged from 0.2 to 0.8% of the ingested dose. The major pathway of metabolism of MeIQx occurred through oxidation of the C⁸-methyl group to form IQx-8-COOH, but the major pathway of PhIP metabolism occurred through oxidation of the exocyclic amine group, to form HONH-PhIP. The latter metabolite underwent glucuronidation to form the isomeric *N*-glucuronide conjugates. 4'-HO-PhIP was a minor component, but it was detected in the urine of all subjects, after meat consumption. 4'-HO-PhIP can form at the low ppb concentration in beef cooked well-done (58,59). Hence, the 4'-HO-PhIP present in urine can either be a minor metabolite of PhIP or it may be derived from unaltered 4'-HOPhIP ingested in the cooked beef. The amounts of 4'-HO-PhIP excreted in urine at the 10 h time point of these subjects are minor, and the levels ranged from an equivalent of 0.2 to 1.0% of the ingested dose of PhIP.

The urinary metabolic ratio (MR) is often used as an indirect method of assessing drug metabolizing enzyme activity in vivo (60). We observed that the extent of MeIQx and PhIP metabolism and the MR (% dose of urinary metabolite/% dose of unmetabolized urinary HAA) for several oxidative urinary metabolites of MeIQx and PhIP were correlated for a given subject. The Spearman's rank correlation coefficient for the percentage of the dose eliminated in urine as unmetabolized MeIQx and PhIP was $r_s = 0.86$. The correlation coefficient relating the MR of the two major oxidative metabolites of MeIQx and PhIP, IQx-8-COOH/MeIQx and HON-PhIP-*N*²-Gl/PhIP, was $r_s = 0.92$; the correlation for IQx-8-COOH/MeIQx and HON-PhIP-*N*³-Gl/PhIP was $r_s = 0.78$; the correlation for IQx-8-COOH/MeIQx and 8-CH₂OH-IQx/MeIQx was $r_s = 0.60$; and the correlation for HON-PhIP-*N*³-Gl/PhIP and HON-PhIP-*N*²-Gl/PhIP was $r_s = 0.90$. These correlations were all significant (p value two-tailed $\alpha < 0.05$), except for the correlation of the MR relating IQx-8-COOH/MeIQx and 8-CH₂OHIQx/MeIQx ($r_s = 0.64$, P value $\alpha = 0.054$) (Figure 7). The inter-relationship between these latter two metabolites could be obscured because P450 1A2 catalyzes the further oxidation of IQx-8-CH₂OH to form IQx-8-COOH (30).

Indirect Measurement of Phase II Detoxification Products of MeIQx and PhIP

MeIQx-*N*²-SO₃H, MeIQx-*N*²-Gl, and HON-MeIQx-*N*²-Gl did not bind to the mixed-mode reversed phase-cation exchange SPE resin. The poor binding of the sulfamate was not surprising, given the compound's strong polarity and negative charge. MeIQx-*N*²-Gl and HON-MeIQx-*N*²-Gl did bind to the SPE resin, when applied as pure standards in 1.8% HCO₂H. However, the binding of the metabolites to the SPE resin was poor, when applied in acidified urine, regardless of pre-processing of the urine samples by organic precipitation, to remove salt and protein. The poor binding of these two MeIQx glucuronide conjugates was unexpected, given that the pK_a values for MeIQx (pK_a 5.94) and PhIP (pK_a 5.65) are similar (61), and given that the binding of the urinary glucuronide metabolites of PhIP to the SPE resin was satisfactory.

Acid hydrolysis of MeIQx-*N*²-SO₃H and MeIQx-*N*²-Gl quantitatively transforms these conjugates to MeIQx (62). The increase in the amount of MeIQx, after acid hydrolysis of urine, was used as a means to estimate the contribution of *N*²-sulfamation and *N*²-glucuronidation to the metabolism of MeIQx (24,62). We concurrently measured, following acid treatment, the amounts of PhIP and the 4'-HO-PhIP; this latter metabolite can undergo further metabolism to form 4'-sulfate or 4'-glucuronide conjugates (18,27). The LC-ESI/MS/MS traces of MeIQx, PhIP, and 4'-HO-PhIP in urine from a subject who ate meat, before

and after acid hydrolysis of urine, are shown in Supporting Information (Figure S-4). The SPE procedure is highly effective in purifying these HAAs from acidified urine: the acid hydrolysis treatment increased the amounts of all of three biomarkers. The contribution of phase II conjugation, to the metabolism of MeIQx and PhIP in urine samples from four subjects, is summarized in Figure 8. The amounts of MeIQx, PhIP and 4'-HO-PhIP increased by 3 to 5-fold, following acid hydrolysis. Approximately 8 – 13% of the ingested dose of MeIQx was present as phase II conjugates, but <3% of the ingested dose was recovered as PhIP or 4'-HO-PhIP, following acid hydrolysis.

The pretreatment of urine with a mixture of β -glucuronidase and arylsulfatase did not increase the urinary concentration of MeIQ because both MeIQx- N^2 -SO₃H and MeIQx- N^2 -Gl are resistant to these hydrolytic enzymes (37). The isomeric PhIP- N -Gl conjugates are poor substrates of β -glucuronidase, whereas β -glucuronidase treatment of urine resulted in complete hydrolysis of HONPhIP- $N3$ -Gl, but HON-PhIP- N^2 -Gl remained intact (data not shown). The relative susceptibilities of these glucuronide conjugates of PhIP to β -glucuronidase are consistent with a previous observation (63). We did observe a modest ~2.5-fold increase in the urinary concentrations of PhIP and 4'-HO-PhIP, following enzyme hydrolysis with a combination of arylsulfatase and β -glucuronidase (data not shown). The amount of the isomeric PhIP- N^2 -Gl conjugate present in urine samples was just at the LOQ (~50 pg/mL), whereas the level of PhIP- $N3$ -Gl was below the LOQ (Figure 5). These findings demonstrate that direct phase II conjugation is more important for the detoxification of MeIQx than for the detoxification of PhIP, in agreement with the findings of a previous study (24).

Discussion

A facile, one-step SPE enrichment procedure was devised to isolate MeIQx and PhIP, and several of their principal metabolites, in urine of omnivores. With this clean-up procedure, twenty urine samples can be processed in one day. Both HAAs undergo extensive metabolism. In the case of MeIQx, the major urinary metabolite is IQx-8-COOH, a detoxification product (31). The primary metabolite of PhIP is HON-PhIP- N^2 -Gl, a conjugate of HONH-PhIP, which is a genotoxic metabolite that covalently adducts to DNA (64). The formation of both IQx-8-COOH (30,31) and HONH-PhIP (14,16) is catalyzed by P450 1A2. Thus, P450 1A2 serves a dual role in the metabolism of HAAs: it catalyzes both the bioactivation and detoxification of MeIQx, but it only catalyzes the bioactivation of PhIP.

Comprehensive analyses of urinary metabolites of MeIQx and PhIP in humans are limited to studies that have employed ¹⁴C-labeled compounds (23,27,43). In a pilot study, five volunteers who were about to undergo colorectal cancer surgery, were given the dietary equivalent of ¹⁴C-labeled MeIQx in a capsule (23). Between 20 and 59% of the ingested dose of MeIQx was excreted in urine within 26 h. Unmetabolized MeIQx and the five principal urinary metabolites were estimated by HPLC with liquid scintillation counting. The estimates of MeIQx and the formed metabolites were (noted as the range in percentages of the ingested dose): MeIQx (0.7- 2.8%); MeIQx- N^2 -SO₃H (0.6 – 3.1%); 8-CH₂OH-IQx (1.0 – 4.4%); MeIQx- N^2 -Gl (1.6 – 6.3%), HON-MeIQx- N^2 -Gl (1.4 – 10.0%); and IQx-8-COOH (8 - 28%).

In this current study, the rates of metabolism and elimination of MeIQx in healthy subjects ingesting MeIQx in well-done cooked beef were greater than the rates determined in the subjects who underwent colorectal surgery; this discrepancy may be reflective of the poorer health status of those subjects (23). We estimated, by LC-ESI/MS/MS, that from 60 to 85% of the ingested dose of MeIQx was eliminated in urine of our healthy subjects, as a

combination of unaltered MeIQx, P450 1A2 derived metabolites, and phase II conjugates, within 10 h of consumption of cooked beef (Table 2). IQx-8-COOH and 8-CH₂OH-IQx (30,31) combined accounted for 34.8 – 76.2% of the ingested dose (Table 2), underscoring the strong contribution of P450 1A2 to the metabolism of MeIQx.

The estimates of unaltered PhIP (0.2 – 0.8% of the dose), as well as the contribution of HONPhIP-*N*²-Gl (14.1 – 29.7% of the dose) and HON-PhIP-*N*3-Gl (1.0 – 3.5% of the dose) to the metabolism of PhIP, are in good agreement to values previously estimated in the 10-h urine samples of these subjects (5), and the estimates of these PhIP metabolites formed are comparable to the data obtained by liquid scintillation counting of radioactivity (27), or by LC-ESI/MS/MS in other feeding studies (26).

The smaller percentage of the dose of PhIP that is eliminated in urine compared to MeIQx, at the 10-h time point of our study, is due to the slower rate of elimination of PhIP: As much as 30 to 50% of the ingested dose of PhIP is excreted in urine between 8 – 48 h post-meat consumption (5,27,43). In human metabolic studies conducted with ¹⁴C-PhIP, the isomeric HON-PhIP-*N*-glucuronide conjugates were reported to account for approximately 50% of the dose eliminated in urine within 24 h, and combined with 4'-HO-PhIP conjugates, PhIP-*N*-Gl, and unaltered PhIP, accounted for 60 – 82% of the dose of PhIP eliminated in urine within 24 h (27). We have also detected, by LC/MS, significant quantities of HON-PhIP-*N*-glucuronide conjugates in urine of our subjects at the 10 to 24-h time point (unpublished observations) (5). Thus, our LC/MS method covers a large proportion of the PhIP dose that is eliminated in urine.

A method was recently developed to measure 2-amino-1-methyl-6-(5-hydroxy)phenylimidazo[4,5-*b*]pyridine (5-HO-PhIP) in urine of omnivores (28). 5-HO-PhIP is a solvolysis product of *N*-acetoxy-PhIP, a penultimate metabolite that reacts with DNA (Scheme 2) (28,40). The analysis of 5-HO-PhIP required heat treatment of urine with hydrazine, under acidic pH conditions, to hydrolyze potential glucuronide conjugates of 5-HO-PhIP, prior to LC/MS (28). The authors estimated high levels of 5-HO-PhIP in human urine, following consumption of meat (28). In a previous study, we did not detect 5-HO-PhIP in urine of omnivores (47), but we did identify several urinary analytes at *m/z* 417.1, an *m/z* that is consistent with the molecular weight of protonated glucuronide conjugates of hydroxylated-PhIP (47). The full scan product ion spectra of these analytes were acquired under elevated collision-induced dissociation conditions to fragment the aglycone ions [M + H – 176]⁺; however, the product ion spectra of these analytes differed from the spectra of either 4'-HO-PhIP or 5-HO-PhIP (47). These urinary components appeared to be isobaric interferences. The major pathways of biotransformation of ¹⁴C-PhIP have been characterized in human urine (27,43) and in human hepatocytes (19): Neither 5-HO-PhIP nor its glucuronide or sulfate conjugates were identified as prominent metabolites. Quantitative LC/MS methods with a stable, isotopically labeled internal standard will be required to determine the amounts of 5-HO-PhIP in urine of omnivores (28).

The prominent role of P450 1A2 in the metabolism of MeIQx and PhIP in humans was previously inferred from a pharmacokinetics study on subjects given furafylline (39), a selective and mechanism-based inhibitor of P450 1A2 (65), prior to consumption of cooked beef. In that study, P450 1A2 was estimated to account for 90% of the elimination of MeIQx and 70% of the elimination of PhIP (39). Consistent with that finding, we previously showed that the pretreatment of human liver microsomes with various amounts of furafylline led to a concentration-dependent inhibition of 8-CH₂OH-IQx, IQx-8-COOH, HONH-MeIQx, and HONH-PhIP formation by up to 95% (16,30). The formation of 8-CH₂OH-IQx and IQx-8-COOH, and the glucuronide conjugates of HONH-MeIQx and HONH-PhIP, was also inhibited to a similar degree in human hepatocytes pretreated with furafylline (19,31).

We examined the extent of MeIQx and PhIP metabolism and compared the urinary MR values for several of their P450 1A2-catalyzed oxidation products. The use of MR values and their correlations must be interpreted with caution. A high urine flow rate can limit the utility of MR in assessment of enzyme metabolizing activity *in vivo*, if the elimination of the parent compound or the metabolite is dependent upon the flow rate of urine (60). In a previous study, the renal clearance of MeIQx and PhIP was reported not to be urine flow-dependent (39). In the present pilot study of 10 subjects, we observed that the renal clearances of MeIQx, 8-CH₂OH-IQx, IQx-8-COOH, HON-PhIP-*N*²-G1, HON-PhIP-*N*²-G1, and 4'-HO-PhIP were independent of urine flow rate (Spearman r_s values < 0.52, two-tailed α , $p > 0.14$, urine volume vs percent dose of biomarkers collected in urine over 10 h), but the elimination of PhIP did appear to be correlated with urine flow output ($r_s = 0.74$, two-tailed α , $p = 0.02$). The urinary MR value relating the two major oxidation metabolites of MeIQx and PhIP, IQx-8-COOH/MeIQx and HON-PhIP-*N*²-G1/PhIP were strongly correlated among the 10 subjects of the study (Figure 7). These correlations support the notion that P450 1A2 is an important enzyme in the metabolism of both procarcinogens *in vivo*. A study on a larger number of subjects will be required before we can firmly establish the MR values and the inter-relationship between P450 1A2-mediated metabolism of MeIQx and that of PhIP.

The large contribution of IQx-8-COOH to the metabolism of MeIQx is unexpected, when the steady-state kinetic parameters of P450 1A2 for the formation of IQx-8-CH₂OH, the precursor to IQx-8-COOH, are considered. Based on kinetic studies with human liver microsomes, the catalytic efficiency of P450 1A2 in the first oxidation step of the 8-methyl group of MeIQx to form IQx-8-CH₂OH (k_{cat}/K_m 0.03, V_{max} 0.1 nmol/min/mg protein, K_m 3.1 μ M) is ~10-fold lower than the catalytic efficiency of P450 1A2 in the production of HONH-MeIQx (k_{cat}/K_m 0.26, V_{max} 3.9 nmol/min/mg of protein, K_m 15 μ M) (30). Thus, we postulate that a portion of the HONH-MeIQx metabolite formed *in vivo* undergoes enzymatic reduction back to MeIQx (66), which ultimately undergoes oxidation at the 8-methyl group to form IQx-8-CH₂OH and IQx-8-COOH (Scheme 1).

HON-MeIQx-*N*²-G1 was not measured, due to its poor binding to the SPE resin. The acid treatment of HON-MeIQx-*N*²-G1 produces the deaminated derivative 2-hydroxy-3,8-dimethylimidazo[4,5-*f*]quinoxaline with high yield. This biomarker was employed as an indirect measure of urinary HON-MeIQx-*N*²-G1, by GC/MS (67). HON-MeIQx-*N*²-G1 was deduced to account for $9.4 \pm 3.0\%$ (mean \pm SD) of the dose, and varied in range from 2.2 to 17.1% (mean \pm SD) of the dose in 66 subjects. We observed that 2-hydroxy-3,8-dimethylimidazo[4,5-*f*]quinoxaline also bound poorly to the SPE resin, thus precluding its measurement by our method. Glucuronidation seems to be a less important pathway for the metabolism of HONH-MeIQx than for the metabolism of HONH-PhIP in either humans (23), or in human hepatocytes (31). Further work will be required to develop and optimize the isolation HON-MeIQx-*N*²-G1 from human urine, for its quantification by LC-ESI/MS/MS.

A previous study reported the metabolism of PhIP in wild-type, P450 1A2-null, and P450 1A2-humanized mice in detail, using a metabolomic approach, in which metabolites were characterized by ultraperformance liquid chromatography-time-of-flight mass spectrometry analysis (68). In that study, the dose of PhIP given to mice was 10 mg/kg, a dose that is about 150,000-fold higher than the dose consumed by humans in our current study. It would be of great interest to determine whether high resolution mass spectrometer instrumentation can be employed to examine the urinary metabolome of HAAs in humans, following consumption of cooked meat.

In summary, we have established a robust SPE method to measure MeIQx and PhIP and several of their major urinary metabolites that are produced by P450 1A2. With this

validated analytical method, we plan to explore the influence of genetic polymorphisms that encode enzymes involved in xenobiotic metabolism, and assess the efficacy of chemoprotective dietary constituents to modulate the metabolism of these two potential human carcinogens.

Supplementary Material

Refer to Web version on PubMed Central for supplementary material.

Acknowledgments

This work was funded by R01CA122320 (D.G and R.J.T.) from the National Cancer Institute and by grant number 2007/58 funded by the World Cancer Research Fund International (D.G., R.J.T., and F.F.K.), and T01009 funded by the Food Standards Agency, UK (N.J.G and B.G.L.). We acknowledge the assistance of the NMR Structural Biology Facility at the Wadsworth Center.

ABBREVIATIONS

MeIQx	2-amino-3,8-dimethylimidazo[4,5- <i>f</i>]quinoxaline
MeIgx	2-amino-1,7-dimethylimidazo[4,5- <i>g</i>]quinoxaline
HONH-MeIQx	<i>N</i> -hydroxy-2-amino-3,8-dimethylimidazo[4,5- <i>f</i>]quinoxaline
8-CH₂OHIQx	2-amino-8-(hydroxymethyl)-3-methylimidazo[4,5- <i>f</i>]quinoxaline
IQx-8-COOH	2-amino-3-methylimidazo[4,5- <i>f</i>]quinoxaline-8-carboxylic acid
MeIQx-<i>N</i>²-GI	<i>N</i> ² -(β-1-glucosiduronyl)-2-amino-3,8-dimethylimidazo[4,5- <i>f</i>]quinoxaline
HON-MeIQx-<i>N</i>²-GI	<i>N</i> ² -(β-1-glucosiduronyl)-2-(hydroxyamino)-3,8-dimethylimidazo[4,5- <i>f</i>]quinoxaline
MeIQx-<i>N</i>²-SO₃H	<i>N</i> ² -(3,8-dimethylimidazo[4,5- <i>f</i>]quinoxalin-2-yl)-sulfamic acid
PhIP	2-amino-1-methyl-6-phenylimidazo[4,5- <i>b</i>]pyridine
HONH-PhIP	<i>N</i> -hydroxy-2-amino-1-methyl-6-phenylimidazo[4,5- <i>b</i>]pyridine
4'-HO-PhIP	2-amino-4'-hydroxy-1-methyl-6-phenylimidazo[4,5- <i>b</i>]pyridine
5-HO-PhIP	2-amino-1-methyl-6-(5-hydroxy)phenylimidazo[4,5- <i>b</i>]pyridine
HON-PhIP-<i>N</i>²-GI	<i>N</i> ² -(β-1-glucosiduronyl)-2-(hydroxyamino)-1-methyl-6-phenylimidazo[4,5- <i>b</i>]pyridine
HON-PhIP-<i>N</i>³-GI	<i>N</i> ³ -(β-1-glucosiduronyl)-2-(hydroxyamino)-1-methyl-6-phenylimidazo[4,5- <i>b</i>]pyridine
PhIP-<i>N</i>²-GI	<i>N</i> ² -(β-1-glucosiduronyl)-2-amino-1-methyl-6-phenylimidazo[4,5- <i>b</i>]pyridine
PhIP-<i>N</i>³-GI	<i>N</i> ³ -(β-1-glucosiduronyl)-2-amino-1-methyl-6-phenylimidazo[4,5- <i>b</i>]pyridine
AMS	accelerator mass spectrometry
FWHM	full width at half maximum
GC-NICI-MS	gas chromatography with negative ion chemical ionization-mass spectrometry
HAAs	heterocyclic aromatic amines

LC/MS	liquid chromatography/mass spectrometry
LC-ESI/MS/MS	liquid chromatography-electrospray ionization/mass spectrometry/ tandem mass spectrometry
LOQ	limit of quantification
MR	metabolic ratio
NATs	<i>N</i> -acetyltransferases
ppb	parts per billion
SPE	solid phase extraction
SRM	selected reaction monitoring
SULTs	sulfotransferases
UGTs	uridine diphosphate glucuronosyltransferases

Reference List

1. Hecht SS. Human urinary carcinogen metabolites: biomarkers for investigating tobacco and cancer. *Carcinogenesis*. 2002; 23:907–922. [PubMed: 12082012]
2. Ross RK, Yuan JM, Yu MC, Wogan GN, Qian GS, Tu JT, Groopman JD, Gao YT, Henderson BE. Urinary aflatoxin biomarkers and risk of hepatocellular carcinoma. *Lancet*. 1992; 339:943–946. [PubMed: 1348796]
3. Walton M, Egner P, Scholl PF, Walker J, Kensler TW, Groopman JD. Liquid chromatography electrospray-mass spectrometry of urinary aflatoxin biomarkers: characterization and application to dosimetry and chemoprevention in rats. *Chem Res. Toxicol*. 2001; 14:919–926. [PubMed: 11453740]
4. Lampe JW, King IB, Li S, Grate MT, Barale KV, Chen C, Feng Z, Potter JD. Brassica vegetables increase and apiaceous vegetables decrease cytochrome P450 1A2 activity in humans: changes in caffeine metabolite ratios in response to controlled vegetable diets. *Carcinogenesis*. 2000; 21:1157–1162. [PubMed: 10837004]
5. Walters DG, Young PJ, Agus C, Knize MG, Boobis AR, Gooderham NJ, Lake BG. Cruciferous vegetable consumption alters the metabolism of the dietary carcinogen 2-amino-1-methyl-6-phenylimidazo[4,5-*b*]pyridine (PhIP) in humans. *Carcinogenesis*. 2004; 25:1659–1669. [PubMed: 15073045]
6. Sugimura T, Wakabayashi K, Nakagama H, Nagao M. Heterocyclic amines: Mutagens/carcinogens produced during cooking of meat and fish. *Cancer Sci*. 2004; 95:290–299. [PubMed: 15072585]
7. Felton, JS.; Jagerstad, M.; Knize, MG.; Skog, K.; Wakabayashi, K. Contents in Foods, Beverages and Tobacco. In: Nagao, M.; Sugimura, T., editors. *Food Borne Carcinogens Heterocyclic Amines*. John Wiley & Sons Ltd.; Chichester, England: 2000. p. 31-71.
8. Fukutome K, Ochiai M, Wakabayashi K, Watanabe S, Sugimura T, Nagao M. Detection of guanine-C8-2-amino-1-methyl-6-phenylimidazo[4,5-*b*]pyridine adduct as a single spot on thin-layer chromatography by modification of the ³²P-postlabeling method. *Jpn. J. Cancer Res*. 1994; 85:113–117. [PubMed: 8144391]
9. Dingley KH, Curtis KD, Nowell S, Felton JS, Lang NP, Turteltaub KW. DNA and protein adduct formation in the colon and blood of humans after exposure to a dietary-relevant dose of 2-amino-1-methyl-6-phenylimidazo[4,5-*b*]pyridine. *Cancer Epidemiol. Biomarkers Prev*. 1999; 8:507–512. [PubMed: 10385140]
10. Friesen MD, Kaderlik K, Lin D, Garren L, Bartsch H, Lang NP, Kadlubar FF. Analysis of DNA adducts of 2-amino-1-methyl-6-phenylimidazo[4,5-*b*]pyridine in rat and human tissues by alkaline hydrolysis and gas chromatography/electron capture mass spectrometry: validation by comparison with ³²P-postlabeling. *Chem. Res. Toxicol*. 1994; 7:733–739. [PubMed: 7696526]

11. Magagnotti C, Pastorelli R, Pozzi S, Andreoni B, Fanelli R, Airoldi L. Genetic polymorphisms and modulation of 2-amino-1-methyl-6-phenylimidazo[4,5-*b*]pyridine (PhIP)-DNA adducts in human lymphocytes. *Int. J. Cancer*. 2003; 107:878–884. [PubMed: 14601045]
12. Gorlewska-Roberts K, Green B, Fares M, Ambrosone CB, Kadlubar FF. Carcinogen-DNA adducts in human breast epithelial cells. *Environ. Mol. Mutagen*. 2002; 39:184–192. [PubMed: 11921188]
13. National Toxicology Program. Report on Carcinogenesis. Eleventh Edition. U.S. Department of Health and Human Services, Public Health Service; Research Triangle Park, N.C.: 2005. 2005
14. Zhao K, Murray S, Davies DS, Boobis AR, Gooderham NJ. Metabolism of the food derived mutagen and carcinogen 2-amino-1-methyl-6-phenylimidazo[4,5-*b*]pyridine (PhIP) by human liver microsomes. *Carcinogenesis*. 1994; 15:1285–1288. [PubMed: 8020169]
15. Hammons GJ, Milton D, Stepps K, Guengerich FP, Kadlubar FF. Metabolism of carcinogenic heterocyclic and aromatic amines by recombinant human cytochrome P450 enzymes. *Carcinogenesis*. 1997; 18:851–854. [PubMed: 9111224]
16. Turesky RJ, Constable A, Richoz J, Varga N, Markovic J, Martin MV, Guengerich FP. Activation of heterocyclic aromatic amines by rat and human liver microsomes and by purified rat and human cytochrome P450 1A2. *Chem. Res. Toxicol*. 1998; 11:925–936. [PubMed: 9705755]
17. Crofts FG, Sutter TR, Strickland PT. Metabolism of 2-amino-1-methyl-6-phenylimidazo[4,5-*b*]pyridine by human cytochrome P4501A1, P4501A2 and P4501B1. *Carcinogenesis*. 1998; 19:1969–1973. [PubMed: 9855011]
18. Alexander, J.; Heidenreich, B.; Reistad, R.; Holme, JA. Metabolism of the food carcinogen 2-amino-1-methyl-6-phenylimidazo[4,5-*b*]pyridine (PhIP) in the rat and other rodents. In: Adamson, RH.; Gustafsson, J-A.; Ito, N.; Nagao, M.; Sugimura, T.; Wakabayashi, K.; Yamazoe, Y., editors. *Heterocyclic amines in cooked foods: Possible human carcinogens*. 23rd Proceedings of the Princess Takamatusu Cancer Society. Princeton Scientific Publishing Co., Inc.; New Jersey: 1995. p. 59-68.
19. Langouët S, Paehler A, Welti DH, Kerriguy N, Guillouzo A, Turesky RJ. Differential metabolism of 2-amino-1-methyl-6-phenylimidazo[4,5-*b*]pyridine in rat and human hepatocytes. *Carcinogenesis*. 2002; 23:115–122. [PubMed: 11756232]
20. Kaderlik KR, Minchin RF, Mulder GJ, Ilett KF, Daugaard-Jenson M, Teitel CH, Kadlubar FF. Metabolic activation pathway for the formation of DNA adducts of the carcinogen 2-amino-1-methyl-6-phenylimidazo[4,5-*b*]pyridine (PhIP) in rat extrahepatic tissues. *Carcinogenesis*. 1994; 15:1703–1709. [PubMed: 8055652]
21. Snyderwine EG, Turesky RJ, Turteltaub KW, Davis CD, Sadrieh N, Schut HA, Nagao M, Sugimura T, Thorgeirsson UP, Adamson RH, Thorgeirsson SS. Metabolism of food-derived heterocyclic amines in nonhuman primates. *Mutat. Res*. 1997; 376:203–210. [PubMed: 9202757]
22. Chen C, Ma X, Malfatti MA, Krausz KW, Kimura S, Felton JS, Idle JR, Gonzalez FJ. A comprehensive investigation of 2-amino-1-methyl-6-phenylimidazo[4,5-*b*]pyridine (PhIP) metabolism in the mouse using a multivariate data analysis approach. *Chem Res. Toxicol*. 2007; 20:531–542. [PubMed: 17279779]
23. Turesky RJ, Garner RC, Welti DH, Richoz J, Leveson SH, Dingley KH, Turteltaub KW, Fay LB. Metabolism of the food-borne mutagen 2-amino-3,8-dimethylimidazo[4,5-*f*]quinoxaline in humans. *Chem. Res. Toxicol*. 1998; 11:217–225. [PubMed: 9544620]
24. Stillwell WG, Kidd L-CKS-B, Wishnok JW, Tannenbaum SR, Sinha R. Urinary excretion of unmetabolized and phase II conjugates of 2-amino-1-methyl-6-phenylimidazo[4,5-*b*]pyridine and 2-amino-3,8-dimethylimidazo[4,5-*f*]quinoxaline in humans: Relationship to cytochrome P450 1A2 and *N*-acetyltransferase activity. *Cancer Res*. 1997; 57:3457–3464. [PubMed: 9270013]
25. Strickland PT, Qian Z, Friesen MD, Rothman N, Sinha R. Metabolites of 2-amino-1-methyl-6-phenylimidazo[4,5-*b*]pyridine (PhIP) in human urine after consumption of charbroiled or fried beef. *Mutat. Res*. 2002; 506-507:163–173. [PubMed: 12351156]
26. Kulp KS, Knize MG, Fowler ND, Salmon CP, Felton JS. PhIP metabolites in human urine after consumption of well-cooked chicken. *J. Chromatogr. B Analyt. Technol. Biomed. Life Sci*. 2004; 802:143–153.
27. Malfatti MA, Dingley KH, Nowell-Kadlubar S, Ubick EA, Mulakken N, Nelson D, Lang NP, Felton JS, Turteltaub KW. The urinary metabolite profile of the dietary carcinogen 2-amino-1-

- methyl-6-phenylimidazo[4,5-*b*]pyridine is predictive of colon DNA adducts after a low-dose exposure in humans. *Cancer Res.* 2006; 66:10541–10547. [PubMed: 17079477]
28. Frandsen H. Biomonitoring of urinary metabolites of 2-amino-1-methyl-6-phenylimidazo[4,5-*b*]pyridine (PhIP) following human consumption of cooked chicken. *Food Chem Toxicol.* 2008; 46:3200–3205. [PubMed: 18692111]
 29. Schut HA, Snyderwine EG. DNA adducts of heterocyclic amine food mutagens: implications for mutagenesis and carcinogenesis. *Carcinogenesis.* 1999; 20:353–368. [PubMed: 10190547]
 30. Turesky RJ, Parisod V, Huynh-Ba T, Langouët S, Guengerich FP. Regioselective differences in C(8)- and N-oxidation of 2-amino-3,8-dimethylimidazo[4,5-*f*]quinoxaline by human and rat liver microsomes and cytochromes P450 1A2. *Chem. Res. Toxicol.* 2001; 14:901–911. [PubMed: 11453738]
 31. Langouët S, Welti DH, Kerriguy N, Fay LB, Huynh-Ba T, Markovic J, Guengerich FP, Guillouzo A, Turesky RJ. Metabolism of 2-amino-3,8-dimethylimidazo[4,5-*f*]quinoxaline in human hepatocytes: 2-amino-3-methylimidazo[4,5-*f*]quinoxaline-8-carboxylic acid is a major detoxification pathway catalyzed by cytochrome P450 1A2. *Chem. Res. Toxicol.* 2001; 14:211–221. [PubMed: 11258970]
 32. Wallin H, Mikalsen A, Guengerich FP, Ingelman-Sundberg I, Solberg KE, Rossland OJ, Alexander J. Differential rates of metabolic activation and detoxification of the food mutagen 2-amino-1-methyl-6-phenylimidazo[4,5-*b*]pyridine by different cytochrome P450 enzymes. *Carcinogenesis.* 1990; 11:489–492. [PubMed: 2311193]
 33. Ozawa S, Nagata K, Yamazoe Y, Kato R. Formation of 2-amino-3-methylimidazo[4,5-*f*]quinoline- and 2-amino-3,8-dimethylimidazo[4,5-*f*]quinoxaline-sulfamates by cDNA-expressed mammalian phenol sulfotransferases. *Jpn. J. Cancer Res.* 1995; 86:264–269. [PubMed: 7744696]
 34. Nowell SA, Massengill JS, Williams S, Radomska-Pandya A, Tephly TR, Cheng Z, Strassburg CP, Tukey RH, MacLeod SL, Lang NP, Kadlubar FF. Glucuronidation of 2-hydroxyamino-1-methyl-6-phenylimidazo[4,5-*b*]pyridine by human microsomal UDP-glucuronosyltransferases: identification of specific UGT1A family isoforms involved. *Carcinogenesis.* 1999; 20:1107–1114. [PubMed: 10357796]
 35. Malfatti MA, Felton JS. Human UDP-glucuronosyltransferase 1A1 is the primary enzyme responsible for the N-glucuronidation of N-hydroxy-PhIP in vitro. *Chem. Res. Toxicol.* 2004; 17:1137–1144. [PubMed: 15310245]
 36. Dellinger RW, Chen G, Blevins-Primeau AS, Krzeminski J, Amin S, Lazarus P. Glucuronidation of PhIP and N-OH-PhIP by UDP-glucuronosyltransferase 1A10. *Carcinogenesis.* 2007; 28:2412–2418. [PubMed: 17638922]
 37. Turesky RJ, Bracco-Hammer I, Markovic J, Richli U, Kappeler A-M, Welti DH. The contribution of N-oxidation to the metabolism of the food-borne carcinogen 2-amino-3,8-dimethylimidazo[4,5-*f*]quinoxaline in rat hepatocytes. *Chem. Res. Toxicol.* 1990; 3:524–535. [PubMed: 2103323]
 38. Keating GA, Bogen KT. Estimates of heterocyclic amine intake in the US population. *J. Chromatogr. B Analyt. Technol. Biomed. Life Sci.* 2004; 802:127–133.
 39. Boobis AR, Lynch AM, Murray S, de la Torre R, Solans A, Farré M, Segura J, Gooderham NJ, Davies DS. CYP1A2-catalyzed conversion of dietary heterocyclic amines to their proximate carcinogens is their major route of metabolism in humans. *Cancer Res.* 1994; 54:89–94. [PubMed: 8261468]
 40. Alexander J, Reistad R, Hegstad S, Frandsen H, Ingebrigtsen K, Paulsen JE, Becher G. Biomarkers of exposure to heterocyclic amines: approaches to improve the exposure assessment. *Food Chem. Toxicol.* 2002; 40:1131–1137. [PubMed: 12067575]
 41. Holland RD, Taylor J, Schoenbachler L, Jones RC, Freeman JP, Miller DW, Lake BG, Gooderham NJ, Turesky RJ. Rapid biomonitoring of heterocyclic aromatic amines in human urine by tandem solvent solid phase extraction liquid chromatography electrospray ionization mass spectrometry. *Chem. Res. Toxicol.* 2004; 17:1121–1136. [PubMed: 15310244]
 42. Stillwell WG, Turesky RJ, Sinha R, Skipper PL, Tannenbaum SR. Biomonitoring of heterocyclic aromatic amine metabolites in human urine. *Cancer Lett.* 1999; 143:145–148. [PubMed: 10503894]

43. Malfatti MA, Kulp KS, Knize MG, Davis C, Massengill JP, Williams S, Nowell S, MacLeod S, Dingley KH, Turteltaub KW, Lang NP, Felton JS. The identification of [2-¹⁴C]2-amino-1-methyl-6-phenylimidazo[4,5-*b*]pyridine metabolites in humans. *Carcinogenesis*. 1999; 20:705–713. [PubMed: 10223203]
44. Frandsen H. Deconjugation of N-glucuronide conjugated metabolites with hydrazine hydrate--biomarkers for exposure to the food-borne carcinogen 2-amino-1-methyl-6-phenylimidazo[4,5-*b*]pyridine (PhIP). *Food Chem Toxicol*. 2007; 45:863–870. [PubMed: 17184892]
45. Stillwell WG, Sinha R, Tannenbaum SR. Excretion of the N(2)-glucuronide conjugate of 2-hydroxyamino-1-methyl-6-phenylimidazo[4,5-*b*]pyridine in urine and its relationship to CYP1A2 and NAT2 activity levels in humans. *Carcinogenesis*. 2002; 23:831–838. [PubMed: 12016157]
46. Kidd LC, Stillwell WG, Yu MC, Wishnok JS, Skipper PL, Ross RK, Henderson BE, Tannenbaum SR. Urinary excretion of 2-amino-1-methyl-6-phenylimidazo[4,5-*b*]pyridine (PhIP) in White, African-American, and Asian-American men in Los Angeles County. *Cancer Epidemiol. Biomarkers Prev*. 1999; 8:439–445. [PubMed: 10350440]
47. Fede JM, Thakur AP, Gooderham NJ, Turesky RJ. Biomonitoring of 2-amino-1-methyl-6-phenylimidazo[4,5-*b*]pyridine (PhIP) and its carcinogenic metabolites in urine. *Chem Res. Toxicol*. 2009; 22:1096–1105. [PubMed: 19441775]
48. Turesky RJ, Aeschbacher HU, Malnoe A, Würzner HP. Metabolism of the food-borne mutagen/carcinogen 2-amino-3,8-dimethylimidazo[4,5-*f*]quinoxaline in the rat: assessment of biliary metabolites for genotoxicity. *Food Chem. Toxicol*. 1988; 26:105–110. [PubMed: 3366409]
49. Turesky RJ, Markovic J, Bracco-Hammer I, Fay LB. The effect of dose and cytochrome P450 induction on the metabolism and disposition of the food-borne carcinogen 2-amino-3,8-dimethylimidazo[4,5-*f*]quinoxaline. *Carcinogenesis*. 1991; 12:1847–1855. [PubMed: 1934266]
50. Turesky RJ, Lang NP, Butler MA, Teitel CH, Kadlubar FF. Metabolic activation of carcinogenic heterocyclic aromatic amines by human liver and colon. *Carcinogenesis*. 1991; 12:1839–1845. [PubMed: 1934265]
51. Murray S, Lake BG, Gray S, Edwards AJ, Springall C, Bowey EA, Williamson G, Boobis AR, Gooderham NJ. Effect of cruciferous vegetable consumption on heterocyclic aromatic amine metabolism in man. *Carcinogenesis*. 2001; 22:1413–1420. [PubMed: 11532863]
52. Mottier P, Hammel YA, Gremaud E, Guy PA. Quantitative high-throughput analysis of 16 (fluoro)quinolones in honey using automated extraction by turbulent flow chromatography coupled to liquid chromatography-tandem mass spectrometry. *J Agric. Food Chem*. 2008; 56:35–43. [PubMed: 18078314]
53. Guy PA, Gremaud E, Richoz J, Turesky RJ. Quantitative analysis of mutagenic heterocyclic aromatic amines in cooked meat using liquid chromatography-atmospheric pressure chemical ionisation tandem mass spectrometry. *J. Chromatogr. A*. 2000; 883:89–102. [PubMed: 10910203]
54. Turesky RJ, Goodenough AK, Ni W, McNaughton L, LeMaster DM, Holland RD, Wu RW, Felton JS. Identification of 2-amino-1,7-dimethylimidazo[4,5-*g*]quinoxaline: an abundant mutagenic heterocyclic aromatic amine formed in cooked beef. *Chem Res. Toxicol*. 2007; 20:520–530. [PubMed: 17316027]
55. Werner E, Heilier JF, Ducruix C, Ezan E, Junot C, Tabet JC. Mass spectrometry for the identification of the discriminating signals from metabolomics: current status and future trends. *J Chromatogr. B Analyt. Technol. Biomed. Life Sci*. 2008; 871:143–163.
56. Styczynski PB, Blackmon RC, Groopman JD, Kensler TW. The direct glucuronidation of 2-amino-1-methyl-6-phenylimidazo[4,5-*b*]pyridine (PhIP) by human and rabbit liver microsomes. *Chem. Res. Toxicol*. 1993; 6:846–851. [PubMed: 8117924]
57. MacDougall D, Amore FJ, Cox GV, Crosby DG, Estes FL, Freeman DH, Gibbs WE, Gordon GE, Keith LH, Lal J, Langner RR, McClelland NI, Phillips WF, Pojasek RB, Sievers RE. Guidelines for data acquisition and data quality evaluation in environmental chemistry. *Anal. Chem*. 1980; 52:2242–2249.
58. Kurosaka R, Wakabayashi K, Ushiyama H, Nukaya H, Arakawa N, Sugimura T, Nagao M. Detection of 2-amino-1-methyl-6-(4-hydroxyphenyl)imidazo[4,5-*b*]pyridine in broiled beef. *Jpn. J Cancer Res*. 1992; 83:919–922. [PubMed: 1429200]

59. Reistad R, Rossland OJ, Latva-Kala KJ, Rasmussen T, Vikse R, Becher G, Alexander J. Heterocyclic aromatic amines in human urine following a fried meat meal. *Food Chem. Toxicol.* 1997; 35:945–955. [PubMed: 9463528]
60. Miners JO, Osborne NJ, Tonkin AL, Birkett DJ. Perturbation of paracetamol urinary metabolic ratios by urine flow rate. *Br. J Clin Pharmacol.* 1992; 34:359–362. [PubMed: 1457270]
61. Mendonsa SD, Hurtubise RJ. Determination of ionization constants of heterocyclic aromatic amines using capillary zone electrophoresis. *J Chromatogr A.* 1999; 841:239–247.
62. Stillwell WG, Turesky RJ, Gross GA, Skipper PL, Tannenbaum SR. Human urinary excretion of sulfamate and glucuronide conjugates of 2-amino-3,8-dimethylimidazo[4,5-f]quinoxaline (MeIQx). *Cancer Epidemiol. Biomarkers Prev.* 1994; 3:399–405. [PubMed: 7920207]
63. Kaderlik KR, Mulder GJ, Turesky RJ, Lang NP, Teitel CH, Chiarelli MP, Kadlubar FF. Glucuronidation of *N*-hydroxy heterocyclic amines by human and rat liver microsomes. *Carcinogenesis.* 1994; 15:1701.
64. Lin D, Kaderlik KR, Turesky RJ, Miller DW, Lay JO Jr, Kadlubar FF. Identification of *N*-(Deoxyguanosin-8-yl)-2-amino-1-methyl-6-phenylimidazo [4,5-b]pyridine as the major adduct formed by the food-borne carcinogen, 2-amino-1-methyl-6-phenylimidazo[4,5-b]pyridine, with DNA. *Chem. Res. Toxicol.* 1992; 5:691–697. [PubMed: 1446011]
65. Kunze KL, Trager WF. Isoform-selective mechanism-based inhibition of human cytochrome P450 1A2 by furafylline. *Chem. Res. Toxicol.* 1993; 6:649–656. [PubMed: 8292742]
66. King RS, Teitel CH, Shaddock JG, Casciano DA, Kadlubar FF. Detoxification of carcinogenic aromatic and heterocyclic amines by enzymatic reduction of the *N*-hydroxy derivative. *Cancer Lett.* 1999; 143:167–171. [PubMed: 10503898]
67. Stillwell WG, Turesky RJ, Sinha R, Tannenbaum SR. *N*-oxidative metabolism of 2-amino-3,8-dimethylimidazo[4,5-f]quinoxaline (MeIQx) in humans: excretion of the *N*²-glucuronide conjugate of 2-hydroxyamino-MeIQx in urine. *Cancer Res.* 1999; 59:5154–5159. [PubMed: 10537291]
68. Chen C, Ma X, Malfatti MA, Krausz KW, Kimura S, Felton JS, Idle JR, Gonzalez FJ. A comprehensive investigation of 2-amino-1-methyl-6-phenylimidazo[4,5-b]pyridine (PhIP) metabolism in the mouse using a multivariate data analysis approach. *Chem. Res. Toxicol.* 2007; 20:531–542. [PubMed: 17279779]

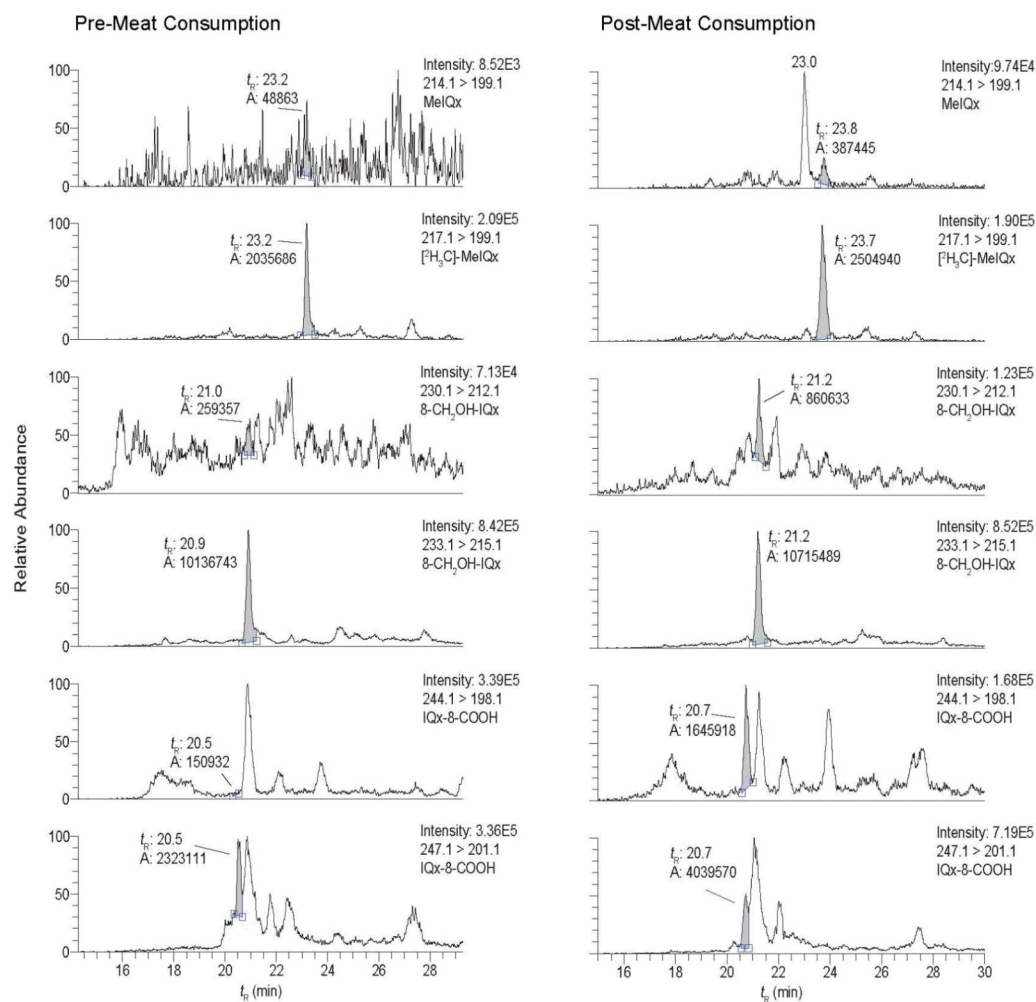


Figure 1.

SRM traces for MeIQx, 8-CH₂OH-IQx, and IQx-8-COOH in a urine sample collected before and after meat consumption. The transition employed to monitor 8-CH₂OH-IQx and IQx-8-COOH, and their internal standards was 20 eV. The retention time (t_R), area, and ion intensity are reported. The large peak eluting at t_R 23.0 min and monitored with the transition 214.1 > 199.1 is 7-MeIQx, an isomer of MeIQx, which elutes at t_R 23.8 min.

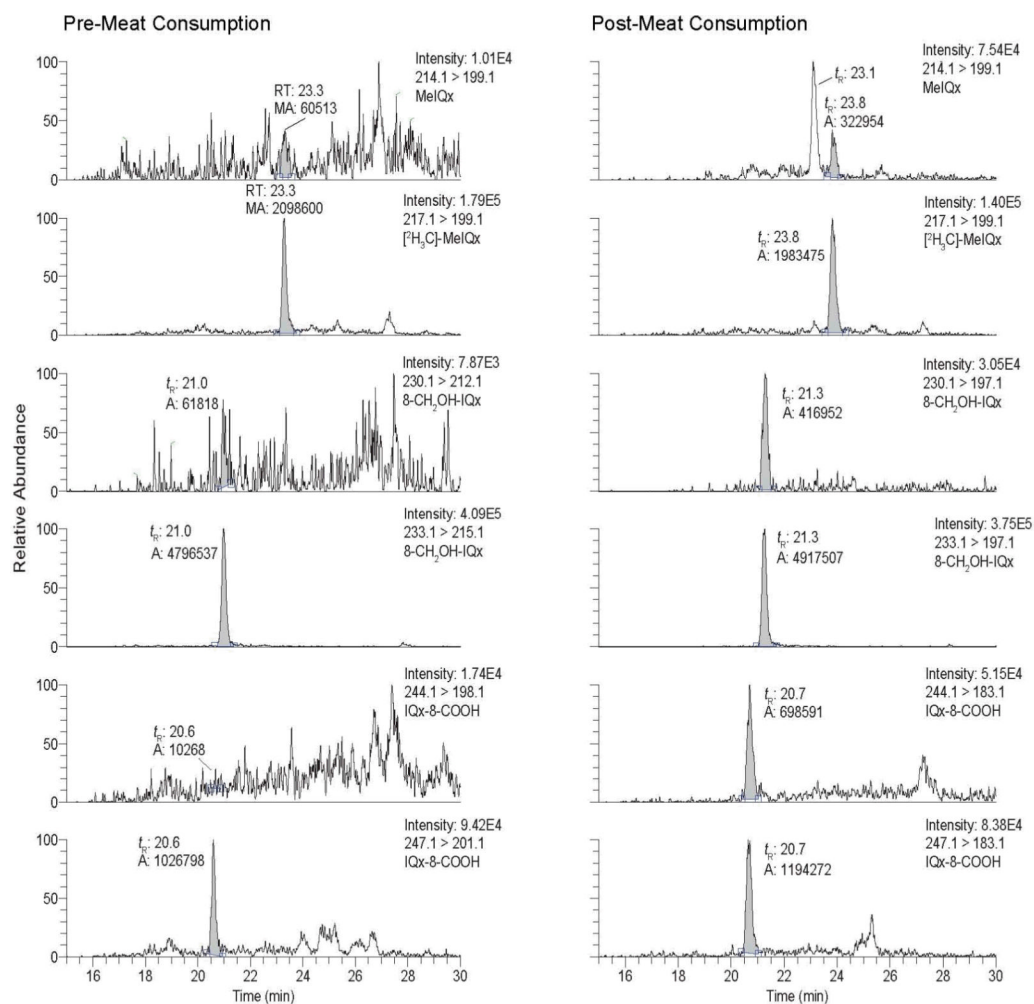


Figure 2. SRM traces for MeIQx, 8-CH₂OH-IQx and IQx-8-COOH in the same urine samples, as in Figure 1, collected before and after meat consumption. The transition employed to monitor 8-CH₂OH-IQx and IQx-8-COOH, and their internal standards was 30 eV.

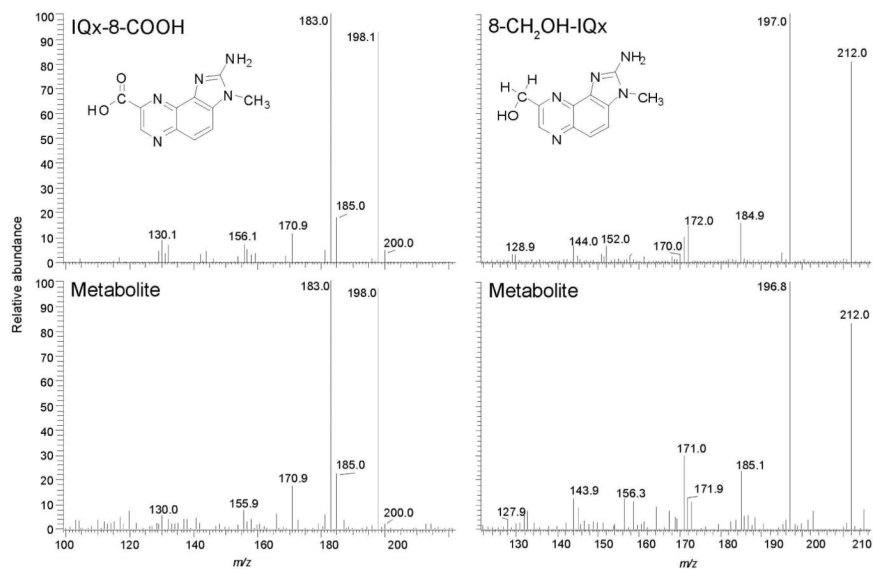


Figure 3. Product ion spectra for the urinary 8-CH₂OH-IQx and 8-IQx-8-COOH metabolites and synthetic compounds (background spectra have been subtracted).

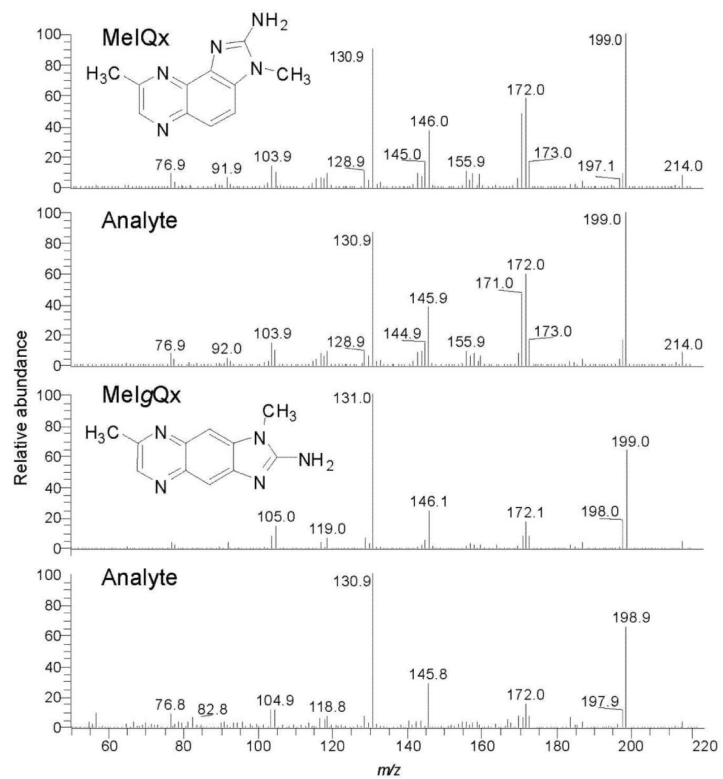


Figure 4. Product ion spectra for MeIQx and MeIqQx in urine following acid hydrolysis (background spectra have been subtracted).

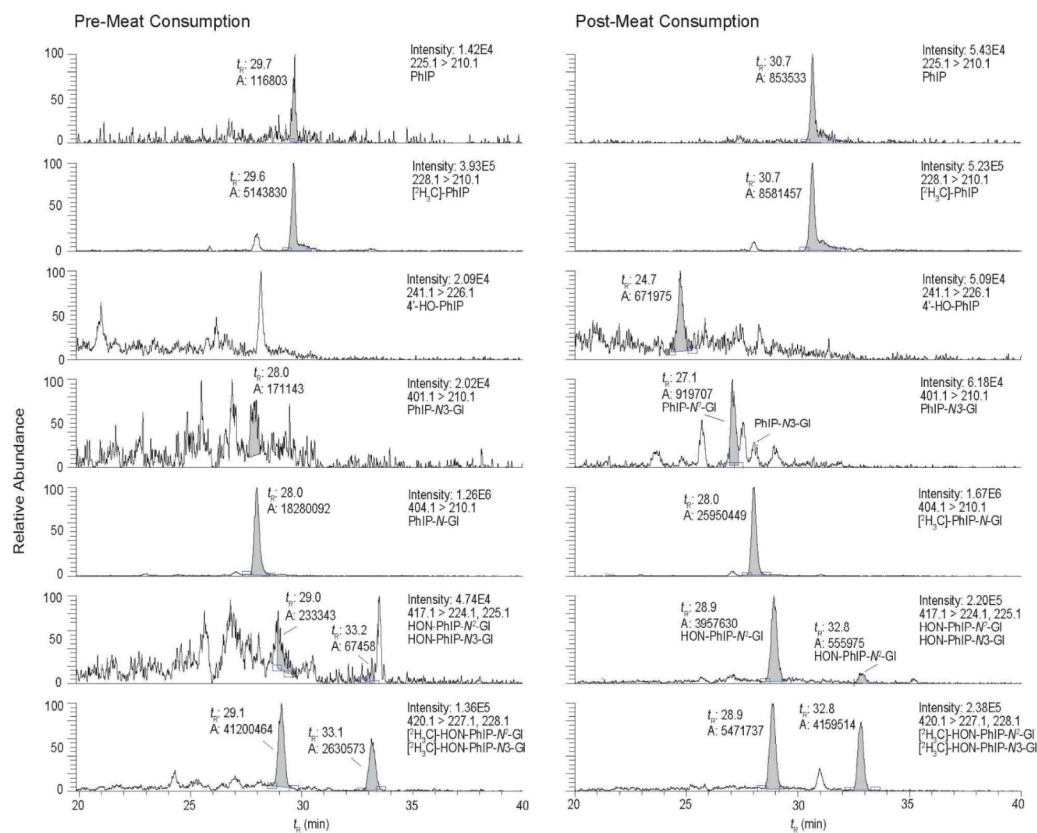


Figure 5. SRM traces for PhIP and its glucuronide metabolites in a human urine sample collected before and after the consumption of cooked beef. The retention time (t_R), area, and ion intensity are reported.

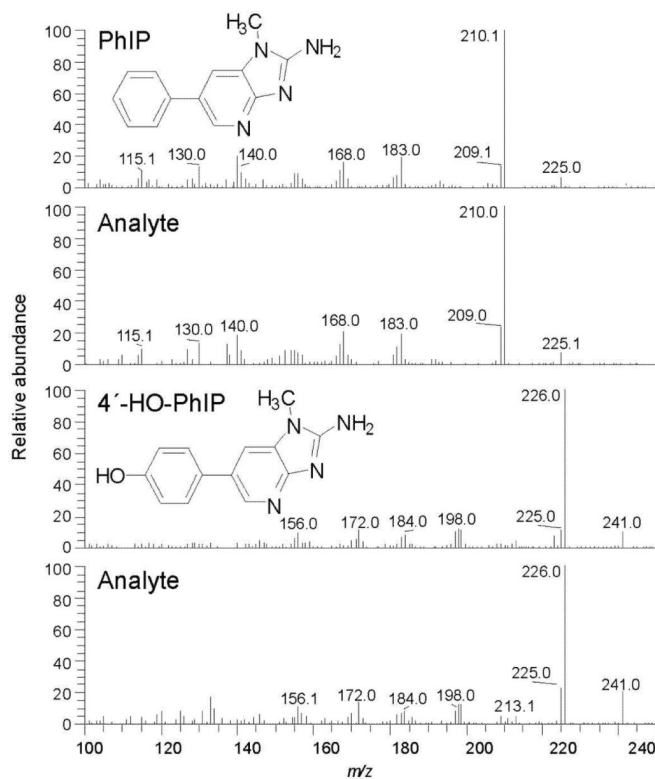


Figure 6. Product ion spectra for PhIP and 4'-HO-PhIP in urine following acid hydrolysis (background spectra have been subtracted).

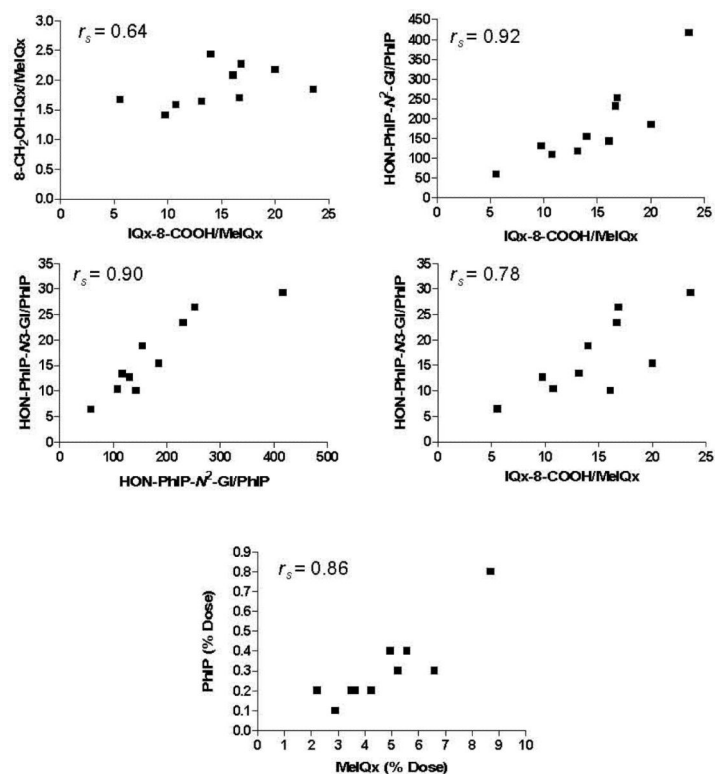


Figure 7.

Scatter plots relating the percentage of the unmetabolized dose of MeIQx and PhIP, and relating the MR of oxidized MeIQx and PhIP metabolites (% of dose of metabolite/% of dose of unmetabolized MeIQx or PhIP) eliminated in urine collected for 10 h after meat consumption.

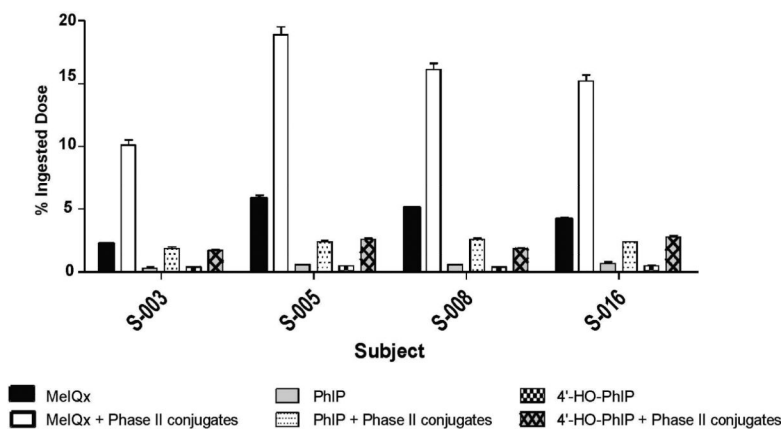
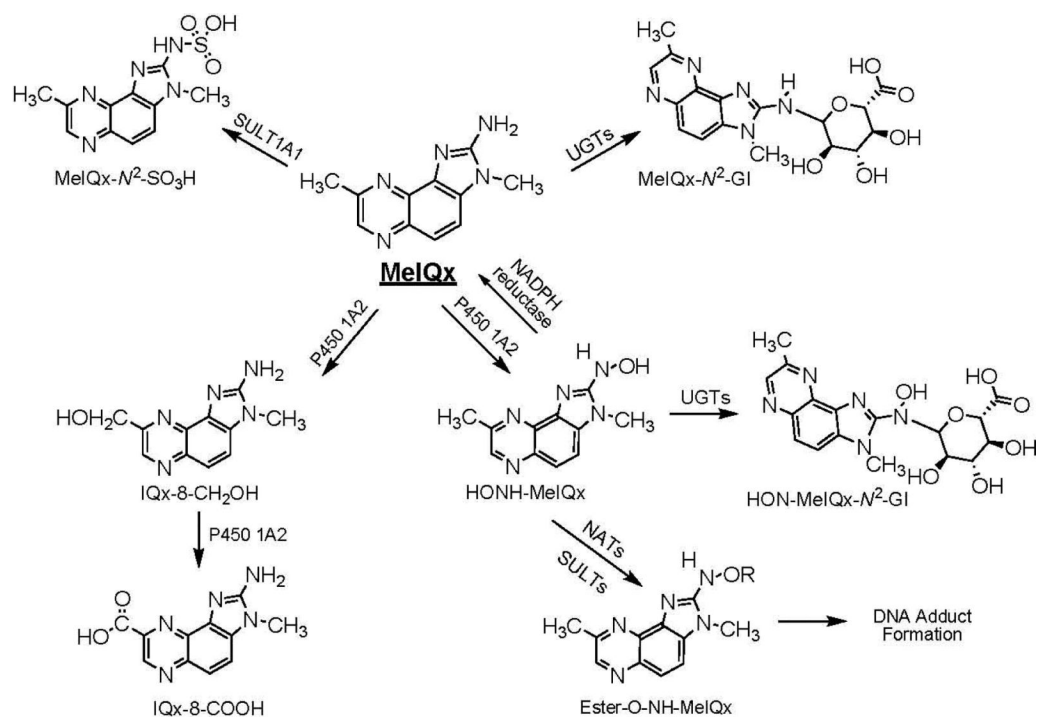
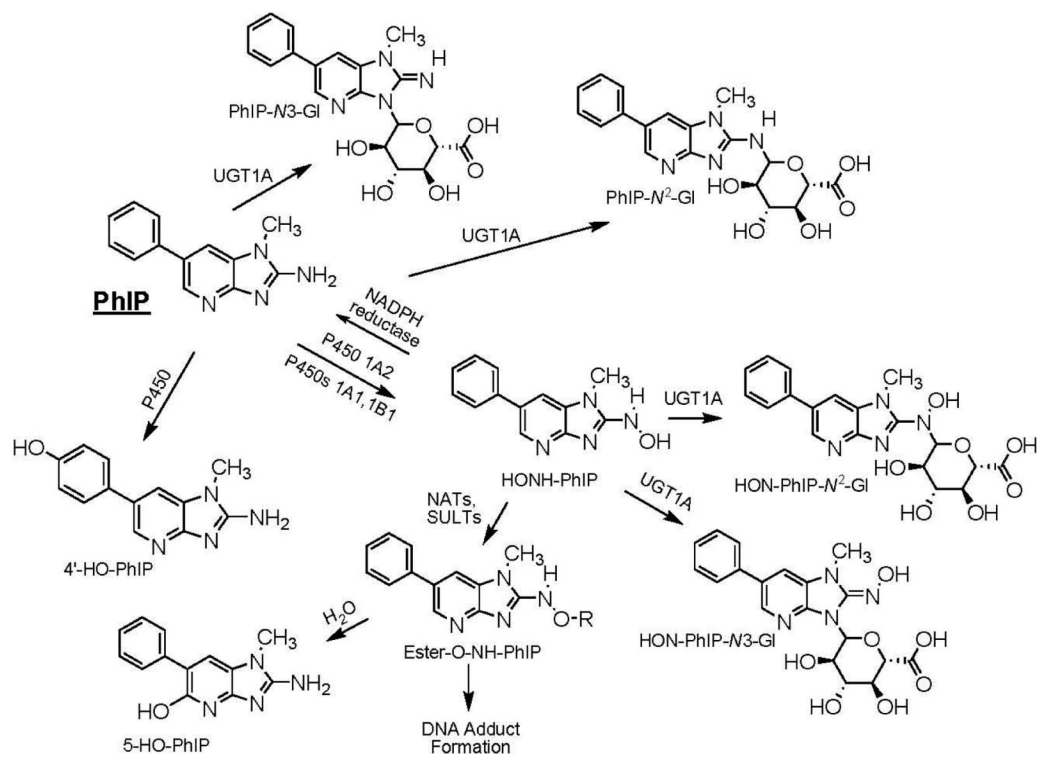


Figure 8.
The contribution of phase II conjugation to the metabolism of MeIQ_x and PhIP in urine samples from four subjects.



Scheme 1.
Major pathways of metabolism of MeIQx in humans



Scheme 2.
Major pathways of metabolism of PhIP in humans.

Table 1

The intraday and interday measurements of MeIQx, 8-CH₂OH-IQx, IQx-8-COOH

Subject	Metabolite	Amount (pg/mL)							CV(%) within-day	CV(%) between-day
		Day 1	Day 2	Day 3	Overall mean					
9	IQx-8-COOH	Mean	237	249	248	245		5.8		
		SD	8.1	19.1	12					
		RSD(%)	3.4	7.7	4.8					
	8-CH ₂ OH-IQx	Mean	34.7	34.6	34.3	34.5		5.1	4.2	
		SD	2.1	1.5	1.4					
		RSD(%)	6.1	4.3	4.1					
	MeIQx	Mean	22.0	22.8	21.5	22.1		4.5	4.8	
		SD	0.8	1.1	1.1					
		RSD(%)	3.6	4.8	5.1					
14	IQx-8-COOH	Mean	179	184	177	180		2.0	2.8	
		SD	3.6	3.2	4.0					
		RSD(%)	2.0	1.7	2.3					
	8-CH ₂ OH-IQx	Mean	23.0	22.9	22.6	22.8		4.4	3.7	
		SD	0.5	1.2	1.1					
		RSD(%)	2.2	5.2	4.9					
	MeIQx	Mean	11.1	10.2	9.9	10.4		5.0	7.2	
		SD	0.6	0.5	0.5					
		RSD(%)	5.4	4.9	5.1					
20	IQx-8-COOH	Mean	395	418	394	402		4.0	4.6	
		SD	164	10.3	20.4					
		RSD(%)	4.2	2.5	5.2					
	8-CH ₂ OH-IQx	Mean	49.0	45.9	43.1	46.0		4.2	7.3	
		SD	1.7	1.0	2.7					
		RSD(%)	3.5	2.2	6.3					

Table 1. Intraday and interday measurements of MeIQx, 8-CH₂OH-IQx, and IQx-8-COOH

Subject	Metabolite	Amount (pg/mL)						
		Day 1	Day 2	Day 3	Overall mean	CV(%) within-day	CV(%) between-day	
	MeIQx	Mean	29.9	29.3	28.5	29.2	4.2	4.2
		SD	0.4	1.3	0.8			
		RSD(%)	1.3	4.4	2.8			

Mean ± SD, n = 3 or 4 replicated per day

Table 2

Measurements of MeIQx and PhIP, and their metabolites in urine collected for 10 h after consumption of cooked beef.

MeIQx		8-CH ₂ OH-IQx		IQx-8-COOH		PhIP		HONH-PhIP-N ² -GI		HONH-PhIP-N ³ -GI		4'-HO-PhIP		
Subject	ng	% Dose	ng	% Dose	ng	% Dose	ng	% Dose	ng	% Dose	ng	% Dose	ng	% Dose
S-001	80.3 ± 2.7	8.7	134 ± 10.4	13.5	447 ± 22.9	42.5	37.1 ± 3.3	0.8	2201 ± 37.3	24.3	238 ± 7.4	2.6	20.1 ± 9.9	0.4
							3.3							
S-003	26.7 ± 1.6	2.9	49.2 ± 2.6	5.0	630 ± 11.6	59.8	6.5 ± 1.1	0.1	2692 ± 121	29.7	189 ± 10.6	2.1	35.0 ± 3.4	0.7
S-005	32.4 ± 1.5	3.5	70.1 ± 5.9	7.1	649 ± 17.8	61.6	11.4 ± 0.9	0.2	2112 ± 88.5	23.3	176 ± 4.2	1.9	41.7 ± 0.9	0.8
S-008	33.8 ± 1.3	3.7	57.4 ± 1.2	5.8	565 ± 25.9	53.6	9.5 ± 0.6	0.2	2198 ± 88.2	24.3	222 ± 10.0	2.5	27.0 ± 3.8	0.5
S-009	45.7 ± 1.4	5.0	72.0 ± 3.8	7.3	493 ± 14.7	46.8	18.5 ± 1.6	0.4	2009 ± 31.0	22.2	191 ± 5.5	2.1	25.2 ± 2.8	0.5
S-012	48.3 ± 1.9	5.2	117 ± 9.0	11.8	678 ± 16.8	64.4	17.0 ± 0.7	0.3	2621 ± 86.0	29.0	319 ± 6.0	3.5	50.1 ± 2.8	1.0
S-013	60.9 ± 3.2	6.6	85.7 ± 4.2	8.6	596 ± 19.7	56.6	14.1 ± 1.2	0.3	1848 ± 25.6	20.4	179 ± 7.0	2.0	37.2 ± 5.2	0.7
S-014	20.6 ± 0.9	2.2	42.8 ± 0.8	4.3	332 ± 5.6	31.5	8.9 ± 0.6	0.2	1274 ± 29.0	14.1	89.5 ± 3.3	1.0	18.4 ± 1.2	0.4
S-015	39.2 ± 2.0	4.2	89.0 ± 6.9	9.0	662 ± 20.5	62.9	8.2 ± 1.0	0.2	2067 ± 103	22.8	216 ± 12.0	2.4	18.3 ± 2.9	0.3
S-020	51.5 ± 2.2	5.6	84.4 ± 2.6	8.5	680 ± 24.3	64.6	18.9 ± 1.6	0.4	2223 ± 15.6	24.6	253 ± 4.9	2.8	38.3 ± 2.5	0.7

Mean ± SD of 3 independent measurements

The estimates of 4'-HO-PhIP were based on the use of [²H₃C]-PhIP as an internal standard and comparable ionization efficiencies were assumed.

We assumed that 4'-HO-PhIP is a metabolite of PhIP and that 4'-HO-PhIP was not formed in cooked beef.